Society for Science and Education
United Kingdom

Journal of Biomedical Engineering and Medical Imaging

Volume 1. Issue 1

TABLE OF CONTENTS

EDITORIAL ADVISORY BOARD

DISCLAIMER

All the contributions are published in good faith and intentions to promote and encourage research activities around the globe. The contributions are property of their respective authors/owners and the journal is not responsible for any content that hurts someone's views or feelings etc.

SOCIETY FOR SCIENCE AND EDUCATION
UNITED KINGDOM

JBEMi JOURNAL OF BIOMEDICAL ENGINEERING AND MEDICAL IMAGING   VOLUME 1, ISSUE 1

Disease modeling – An alert system for informing environmental risk factor for TB infection

K. Ram Mohan Rao*, Yogesh Kant, Kapil Yadav**, Satya Chandra***

**National Remote Sensing Centre, Indian Space Research Organization, Hyderabad, India;*

***Indian Institute of Remote Sensing, Indian Space Research Organization, Dehradun, India;*

krmrao7@gmail.com

ABSTRACT

Tuberculosis (TB) is an infectious disease caused by the bacillus *Mycobacterium tuberculosis* and spreads through air by a person suffering from TB. A risk map is derived based on socio-economic, environmental, health facilities, and Biological characteristics for quantifying the infection risk of the locality. The inter relation between the environmental variables, meteorological parameters, and socio economic variables such as rainfall, temperature, family income and population density with respect to number of past cases have been studied using regression model. Risk is calculated by mean of the probability of occurrence of tuberculosis and vulnerability to the infection. The risk map is computed by using statistical techniques to form spatial maps. An alert system is developed by using GIS from the background of geospatial data and later published to the web using open source internet GIS technologies.

Keywords: Mycobacterium tuberculosis, Regression, vulnerability, GIS.

1. INTRODUCTION

The 1990 World Health Organization (WHO) report on the Global Burden of Disease ranked Tuberculosis (TB) as the seventh most morbidity causing disease in the world, and expected it to continue in the same position up to 2020 [1]. Each year, 8.74 million people develop TB and nearly 2 million die. This means that someone somewhere contracts TB every four seconds and one of them dies every 10 seconds [2]. Unless properly treated, an infectious pulmonary TB (i.e., the TB of lungs) patient can infect 10-15 people in a year [3]. TB is the most common opportunistic disease that affects people infected with HIV. As HIV debilitates the immune system, vulnerability of TB is increased many fold. It is estimated that without HIV, the lifetime risk of TB infected people developing tuberculosis is only 10%, compared to over 50% in the case of people co infected with Human immunodeficiency virus HIV and TB [4]. HIV is also the most powerful risk factor for the progression of TB infection to the disease. In a reciprocal manner, TB accelerates the progression of HIV in to Acquired Immune Deficiency Syndrome

DOI: 10.14738/jbemi.11.81
Publication Date: 15th February 2014
URL: http://dx.doi.org/10.14738/jbemi.11.81

(AIDS), thus shortening the survival of patients with HIV infection. Fortunately, TB is a curable disease even among the HIV infected people. The prevalence of TB and HIV co-infection worldwide is 0.18% and about 8% TB cases have HIV infection [5]. Currently, factors such as booming population, environmental pollution and rapid urbanization in many countries and global warning influence the conditions for disease outbreaks. Disease studies have revealed strong spatial aspects of disease diffusion. Thus, mapping spatial aspects of diseases could help people to understand some puzzles of disease outbreak. Unlike the raw disease data and disease maps offer a visual means of identifying cause and effect relationship existing between humans and their environment. Disease maps can enable health practitioners and the general public to visually communicate about disease distribution.

TB is generally considered to be linked to industrialization and urbanization. Peaking in the 1800 sand receding slowly after, the disease declined sharply in the West after World War II. TB has made a comeback in the last 20 years in developing countries such as China and India. Because socio-economic conditions alone cannot explain the connection between industrialization and TB. Historical statistics on coal consumption and TB disease in Canada, USA and China are correlated. A hypothesis linking TB and air pollution is developed in the context of industrialization. Historical statistics support a hypothesis linking tuberculosis and air pollution caused by coal. Trembla model is proposed whereby triggering of the interleukin-10 (IL-10) cascade by carbon monoxide in lung macrophages promotes the reactivation of Mycobacterium tuberculosis. Remotely sensed data can be used to identify, monitor and evaluate environmental factors between vector and environmental relationships. Recently, Geographic information system (GIS) and remotely sensed data are being used to evaluate and model the relationships between climatic and environmental factors with incidences of viral or bacterial borne diseases. Spatial analysis involves the use of Geographic Information System (GIS) for health that has been reviewed by several authors [6]. Both spatial and temporal changes in environmental condition may be important determinants of vector borne disease transmission. Remote sensing data can be used to provide information on spatial distribution of the vector vector-borne diseases and the physical environment [7]. Wong et al., 2006 presented on development of An Alert System for Informing Environmental Risk of Dengue Infections using Remote Sensing and GIS has discussed on incidence of dengue with the environment and climate [8]. In this study the factors used for analysis are interrelationship between ovitrap index (This is a measurement of mosquito eggs in specified geographic location, which in turn reflects the distribution of Aedine mosquitoes) and temperature. An alert system is created using risk level spatial map of locations. Use of Remote sensing and GIS helped to understand the behaviour of dengue vectors and its inevitable linkages with the environmental factors.

GIS tools have been applied to investigate the spatial relation between malaria risk and distance from breeding sites [9]. However, no attempt has been made to explain, on a larger scale, the existing disease patterns by linking disease incidence data with environmental, population, socioeconomic and entomological features on a GIS platform. Smith 2008 have carried out study on linking the tuberculosis occurrence and environmental pollution due to use of coal and he found that overall coal consumption when compared to TB notification rates, shows an apparent close relationship between global increases in coal consumption and TB disease notification rates [10]. TB incidence and coal use have increased in a similar fashion in the last 20 years, with simultaneous peaks around 1986, 1990 and 1996. However no attempt is made to relate the existing tuberculosis incidence with environmental factors like (temperature, rainfall) population, socioeconomic feature on GIS platform. Mandy Tang and Cheong-wai Tsoi done a study on GIS initiatives in improving the dengue vector control they reviewed the methodology adopted in Hongkong for control of the disease and proposed a GIS based approach to enhance the management and monitoring of the disease, by considering temporal, environmental and climatic factors. For this they used the correlation between ovitrap index and the various meteorological factors such as temperature and rainfall using conventional correlation and regression techniques [11]. This study helped them to understand that the GIS approach can be used to analyze spatial patterns of vector borne diseases. Spatial analysis techniques in a GIS can help determine the most likely areas of mosquito infestation. The GIS techniques can also help understand correlations between climatic factors and vector surveillance data (e.g. ovitrap indices). The use of GIS in disease modeling like tuberculosis requires the relationship between the environmental and meteorological factors with the incidence of disease cases in specific. This study provide social level risk map to improve prevention measures using GIS technologies. The use of RDBMS technologies to link this information with environmental factors and establish a model, and to publish this risk spatial map to web using open source internet GIS technologies.

Geographical Information Systems (GIS) has strong capabilities in mapping and analyzing not only spatial data, but also disease data, and can integrate many kinds of data to greatly enhance disease surveillance. It can render disease data along with other kinds of data like environmental data, representing distribution of contagious disease with various cartographical styles. Meanwhile, the rapid development of the internet technologies influences the popularity of web-based GIS, which itself shows great potential for sharing of disease information through distributed networks. The overall objective of this study is to generate an alert system using GIS modeling for the tuberculosis prone areas based on socio-economic environmental health facilities and individual biological characteristics. The study focuses on generation of the social risk spatial maps for tuberculosis incidences using socio-economic, environmental factors and incidences of Tuberculosis in GIS environment. Finally these spatial risk maps are published on web using open source Internet GIS technologies for the sharing of the risk indices to the general public and governmental agencies.

2. STUDY AREA

Uttarakhand is located in the northern part of India and has a total geographic area of 51,125 sq kms (figure 1). The co-ordinates of Uttarakhand are 28^{o} C 43' N to 31^{o} C 27' N (Latitude) and 77^{o} C 34' E to 81^{o} C 02' E (Longitude). Almost the entire region of Uttarakhand is covered by mountains (approximately 93%) and forests show up on about 64% of the mountains**.** The primary reason for selecting the study area is, in Uttarakhand state there are several cases of tuberculosis, especially in districts like Dheradun and Haridwar according to the performance report of the Revised National Tuberculosis Control Programme (RNTCP) there are more than 1000 cases in Dehradun in the year of 2009 and same in the other districts as well hence, it is meaningful to study about the Uttarakhand area. The spatial data is prepared up to the districts level using administrative data. Individual districts are provided with districts name, total population, income, and number of TB cases in different year.

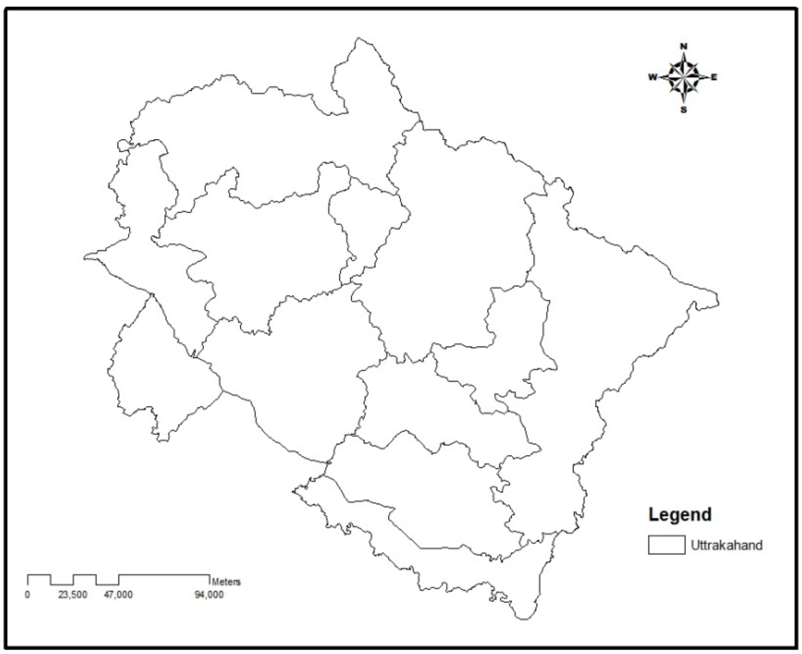

Figure 1: Location of the study area

3. METHODOLOGY

This study is carried out to identify the significant parameters namely socioeconomic indicator of Tuberculosis. Uttarakhand state map is categorized up to the district level along with district name, area, population, past TB cases, meteorological data. Tuberculosis incidence data are collected from the RNTCP (Revised National Tuberculosis Control Programme) performance report of Uttarakhand. This data include information about all suspected and confirmed tuberculosis cases reported during the year 2008 and 2009 for each quarter of the year according to each district in Uttarakhand. Data on average rainfall and temperature is obtained from the websites Indian Meteorological Department. To determine the correlation between socio economic factors and tuberculosis incidences, correlation and regression method is used. Using these parameters and tuberculosis data social risk map is generated. The risk map is then published on web using internet GIS technologies [12]. A general scheme of work flow is given in figure 2.

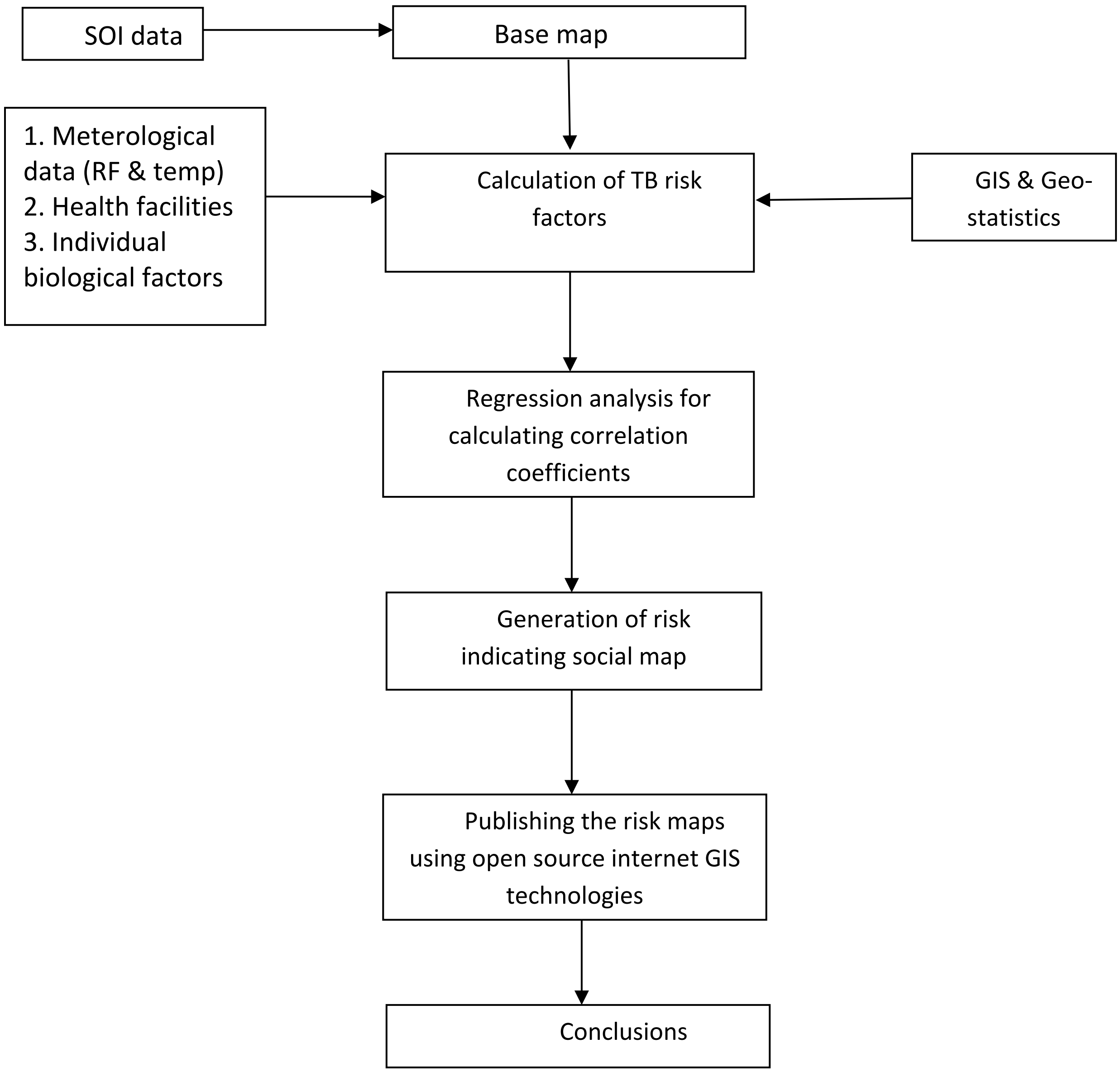

Figure 2: Methodology

Climate data is compared with tuberculosis incidences data to evaluate tuberculosis favorable conditions, because of the reason that Tuberculosis is a disease whose occurrence depends on several environmental and socio-economic variables like temperature, rainfall, population. Surrounding environment, income details based on the previous studies, and knowledge about the occurrence of tuberculosis disease factors used in this study. These factors are related with the occurrence of tuberculosis, and their individual correlation is found to show how much each of them is correlated with disease occurrence.

Now, the risk R is calculated by the formula given by Mohammed et. al given location[13].

$$R= P\times V \text{ .... } (1)$$

Where, P is probability of occurrence of the disease at given location and V is expression of certain context, condition conductive. The probability P is expressed as:

$$P=k_0+k_1*(x_1)+k_2*(x_2)+k_3*(x_3)+k_4*(x_4) \text{ .... } (2).$$

x_1=Temperature data

x_2= Rainfall data

x_3= Population

x_4= Family income

$k_{0,}k_1$,k_2 k_3 and k_4 are correlation coefficients. Similarly vulnerability V represents:

$$V= (Y_1\times Y_2\times Y_3)/Y_4 \text{ .... } (3)$$

Where,

Y_1=Individual biological factors (immuno-deficiency).
Y_2=Social and economic circumstances (crowding, poor nutrition).
Y_3=Environmental and institutional factors (silica dust, pollution).
Y_4=Availability of health facilities.

Correlation and statistical analysis are the major tools used in the study for investing and testing the relation between various parameters and tuberculosis incidences. Various variables like temperature, rainfall, population, and family income are taken in account for analysis. From the various variables the four variables namely temperature, rainfall, income and population that are significantly correlated to tuberculosis incidence are submitted to the multiple regression analysis. In the multivariate case there is more than one independent variables, therefore the regression line cannot be visualized in two dimensional spaces. However, it is possible to construct a linear equation containing all the variables in general multiple regression using the equation.

$$Y=k0+k1*(x1)+k2*(x2)+k3*(x3)+k4*(x4) \text{ ...... } (4)$$

Y=incidence of tuberculosis (dependent variable)

x1=Temperature data

x2= Rainfall data

x3= Population

x4= Family income and $k_{0,}k_1$,k_2 k_3 and k_4 are correlation coefficients.

The regression coefficient represents the independent contribution of each independent variable for the prediction of the dependent variable. Multiple regression analysis was done using the MATLAB tools. Using raster surfaces for each of the independent variables probability surface is generated. Interpolation techniques are used for generation of raster surfaces using correlation parameters for probability surface using raster calculator in Arc GIS. Avaibility of health facilities and individual biological factors like (cases of HIV) is used for generation of vulnerability surface. Since risk is the combination of probability and vulnerability is already defined risk surface is also generated using spatial analyst techniques. The final risk map is published on intranet using Geoserver tool, which is the reference implementation of the Open Geospatial Consortium (OGC) based Internet GIS tool having Web Feature Service (WFS) and Web Coverage Service (WCS) standards, as well as a high performance certified compliant Web Map Service (WMS) [12].

4. RESULTS AND DISCUSSIONS

Using socio-economic, environmental, and individual biological factors probability and vulnerability to the occurrence of tuberculosis maps are generated using GIS technologies. Based on the other factors like temperature, rainfall, population density and family income along with the correlation coefficients for each of the parameter probability of occurrence of tuberculosis is calculated. Raster surface for temperature is created using the krigging interpolation techniques, similarly raster surface is created for the average rainfall values using thiessen polygon interpolation algorithm. Using these surfaces regression coefficients are derived for probability to the occurrence as per the following equation.

$P=2830.8 + (30.30) \times RAIN - (114.6) \times Temperature + (.025) \times Population\ density + (.02) \times Family\ income$……. (5)

Using multiple regression analysis coefficients of multiple determination value for different parameters are calculated (R square) which comes out to be 0.7289 which means that 72.89 % of change in tuberculosis incidences can be explained by the change of independent variables, therefore this analysis is significant at 95% confidence interval. Table 1 shows the coefficients of multiple determination value of the different parameters.

Table 1. Coefficient of multiple determination values

Parameter	R value
Temperature	0.58
Rainfall	0.41
Population	0.09
Income	0.05
HIV	0.42
Overall	0.72

R square for temperature is 0.5681 means 56.81% of change in tuberculosis incidence can be explained by the change in temperature values. Similarly 40.12 % of change in tuberculosis can be explained by the independent change in rainfall values. As it is clear from the R square value of the regression that the independent variables are significantly correlated to the incidences of tuberculosis. Using these correlation coefficients and the raster surface created for all independent variables surface for probability is evaluated using the in Arc GIS software tools. As from the multiple regressions analysis there is significant relationship between actual and predicted values of the tuberculosis incidences. The correlation graph is as shown in the figure 3.

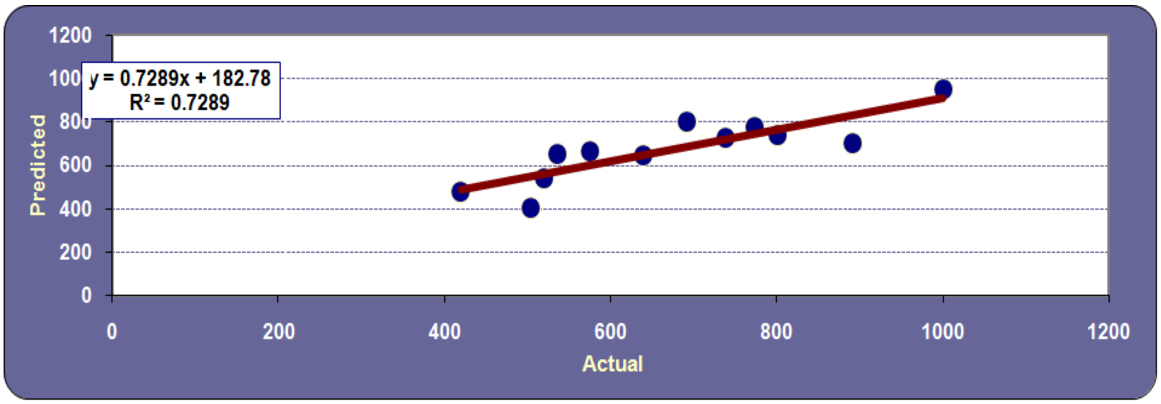

Figure 3. Actual Vs Predicted values of tuberculosis incidences

The probability surface is generated with the inputs of rainfall, population density and family income in a spatial environment. Figure 4 shows the spatial distribution of probability surface generated in GIS environment. The spatial distribution of probability of disease in the state is classified into five categories namely very high, high, moderate, low and very low.

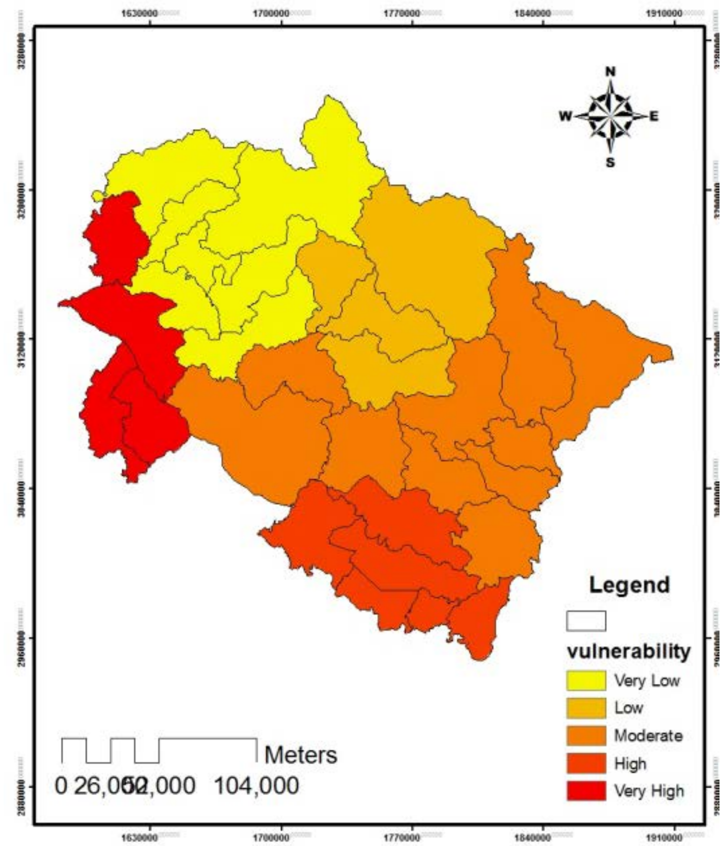

Figure 4: Probability distribution surface.

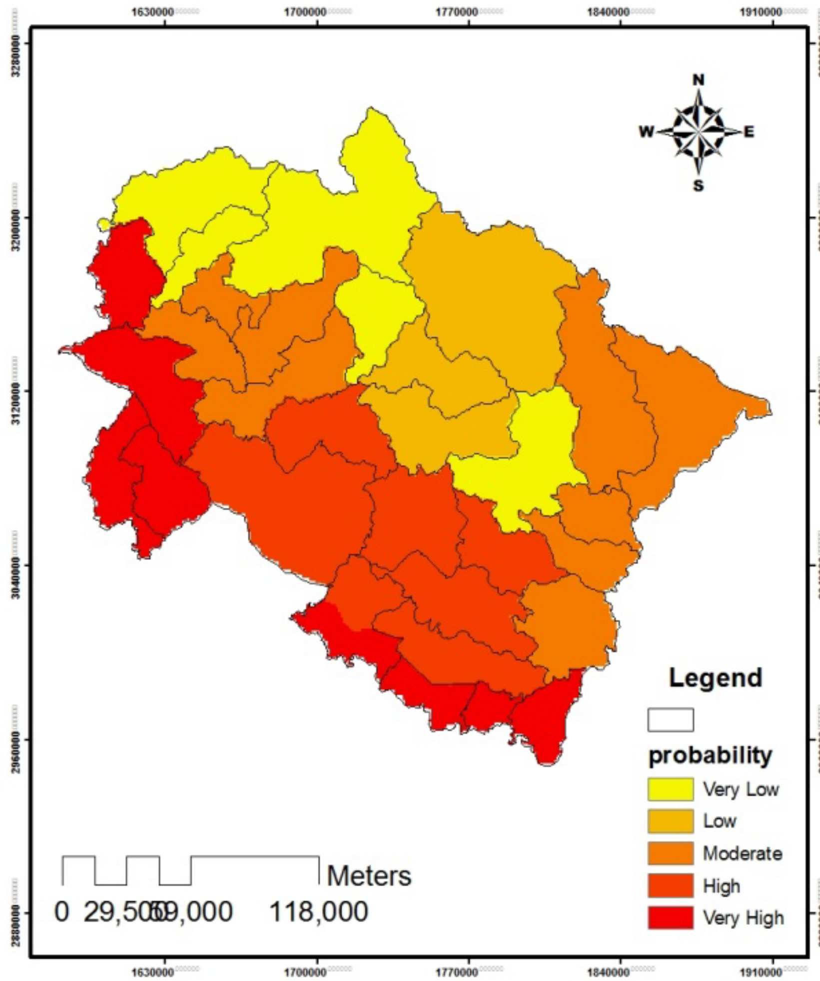

Figure 5: Vulnerability distribution surface

After evaluating the probability surface, vulnerability to the occurrence of tuberculosis is calculated, based on the vulnerability criteria as per the equation 3. Figure 5 shows the vulnerability representation of the Uttarakhand state.

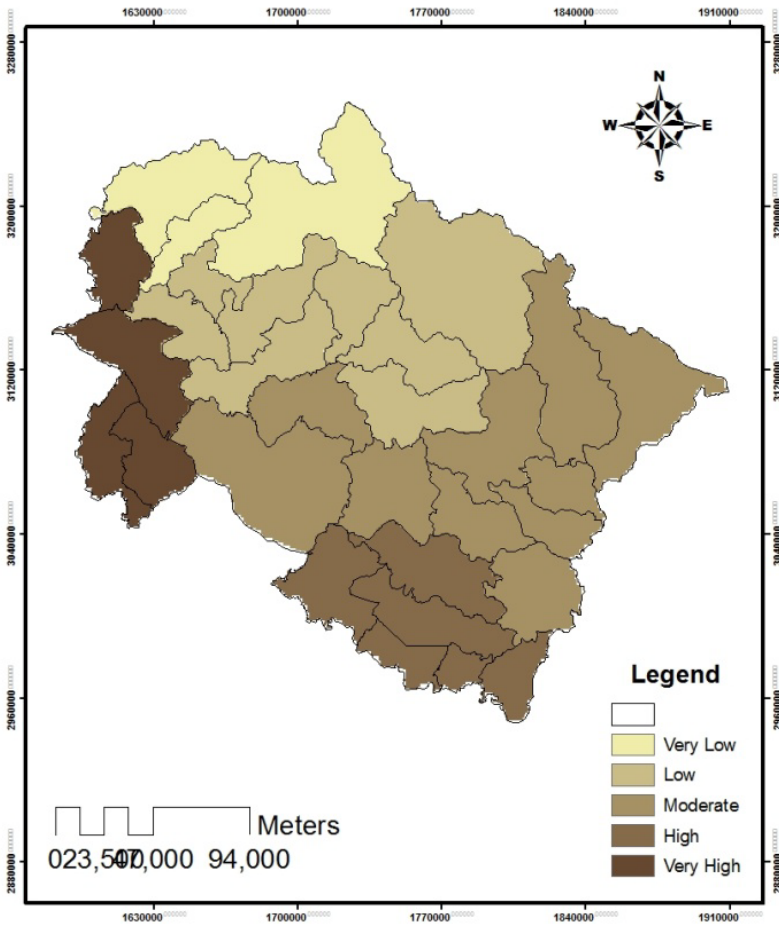

Figure 6. Risk Map for occurrence of tuberculosis in Uttrakhand

Finally the risk values for the tuberculosis are calculated on the basis of equation 1. Like probability and vulnerability surfaces the final risk is also classified in five different classes. Figure 6 shows the final risk values for the tuberculosis distribution on the state of Uttarakhand. According to the risk map obtained, the districts namely Dheradun, Haridwar, Nanital and U.S Nagar are at higher risk to the tuberculosis infection. This is because of the reason that this part of region is having more number of past cases of tuberculosis and highest cases of HIV in the state as compared to other districts, along with other dominant parameters. The temperature value is relatively high in these areas supported by high population density. Districts namely Uttrakashi, Chamoli, Ghrhwal are at low risk to the tuberculosis infections because of low temperature and low population density less number of past cases of tuberculosis. The risk map along with vulnerability and probability parameters are published on the web using open source Geoserver.

5. CONCLUSION

This study demonstrates the use of GIS technologies for disease surveillance which plays a major role in public health and epidemiology. Study also illustrate the spatial statistical analysis can help to identify and visualize potential risk areas of the disease. The criteria to visualize the spatial distribution of the risk to the tuberculosis provide the information on incidences of infections and provide a more objective way of defining risk levels with the aid of GIS unlike the conventional practice of posting statistics about the disease occurrence in tabular formats. This allows visualization of the various variables dependence on occurrence of tuberculosis in association with five risk levels for easy interpretation by the decision makers.

This study illustrates a method for expressing alert warnings in the spatial scale. The use of spatial graphics provide a clearer picture and an easy way to understand the severity or spread of tuberculosis infections which is considered more superior to the data presented in statistical and textual formats. In addition statistical analysis allows the user to explore contribution of the various factors in occurrence of tuberculosis. The study therefore serves as both objective platform for informing risks and a tool for evaluating the influence of various factors on the risk levels.

It is anticipated that the risk alert system can contribute to the prevention of tuberculosis infections in real situations. This can be effective means for of raising awareness of the public in tuberculosis risk. However an effective prevention will require active participations from all the sectors of community and individual family aiming at awareness about the causes of tuberculosis and its prevention.

REFERENCES

[1]. Murray CJL, and Lopez AD: The global burden of disease: a comprehensive assessment of mortality and disability from diseases, injuries and risk factors in 1990 and projected to 2020. World Health Organization Document 1996, W 74 96GL-1/1996.

[2]. Narain JP (ed.): Tuberculosis-epidemiology and control. World Health Organization, Regional Office for South East Asia, New Delhi, India 2002, SEA/TB/2002. 248:15-18.

[3]. India 2005. RNTC Status Report. Central TB Division, Directorate General of Health Services, New Delhi. [http://www.tbcindia.org].

[4]. Cauthen GM, Pio A, and ten Dam HG. Annual risk of infection. World Health Organization Document 1988, WHO/TB/88.154: 1-34.

[5]. Dye C, Scheele S, Dolin P, Pathania V and Raviglione MC.1999. Global burden of disease: estimated incidence, prevalence, and mortality by country. J Am Med Assoc 1999, 282: 677-686.

[6]. Mayer JD. 1986.The role of spatial analysis and geographic data in detection of disease casusation.soc sci med.17:1213-1221.doi:10.1016/0277-9563 (83090014-X.

[7]. Hay SI, Randolph SE, and Rogers DJ. 2000. An overview of remote sensing and Geodesy for Epidemiology and Public Health application..oxford: academic press: .pp 1-35

[8]. Telzak EE. 1997.Tuberculosis and Human Immunodeficiency Virus infection. Med Clin North Am, 81: 345-360.

[9]. Gunawardena,D.M.,wickeremasinghe,A.R.;Muthuwatte, L.; Weerasingha,.1998.Malaria risk factors in an academic region of Srilanka, impact and cost implications of risk-factors based interventions. American Journal of Tropical Medicine and Hygiene 58:533-542

[10]. Smith JM, Miron M, Tremblay T, Ellis E.2008 Burden of Latent Tuberculosis Infection Among Federal Inmates 1998 to 2005. 6th Tuberculosis Conference 2008—Tuberculosis: It's a Small World, Edmonton, Alberta, March, 2008.

[11]. Mandy Tang and Cheong wai Tsoi. 2007. GIS intitiatives in improving the Dengue Vector Control. Eds. Poh. C and Ann S.H. GIS for health and management. Development in the Asia and pacific region. Springer publication.

[12]. Peng ZR, Tsou MH, 2003, Internet GIS: Distributed Geographic Information Services for the internet and wireless networks. ISBN 0-471-35923-8m.

[13]. Mohemmad Zouiten, Mostafa Harti, Chakib Nejjari, 2010. An architecture and an ontology-based context model for GIS health monitoring and alerting: Case of tuberculosis in Morocco. International Journal of Computer Science and Network Security VOL 10. No.11 November 2010;

SOCIETY FOR SCIENCE AND EDUCATION
UNITED KINGDOM

JBEMi JOURNAL OF BIOMEDICAL ENGINEERING AND MEDICAL IMAGING VOLUME 1, ISSUE 1

Nuclear Magnetic Resonance Spectroscopy Studies Of Human Immunoglobulin 'G' In Duchene Muscular Dystrophy

Sanjeev Kumar and Sweety

Department of Physics, Medical Physics Research Laboratory,D.A.V. (P.G.) College, Muzaffar Nagar – 251 001 U.P. (India).

sanjeev1962kumar@yahoo.co.in; sanjeev1962kumar@rediffmail.com

ABSTRACT

In the present paper, we have studied human Immunoglobulin G (IgG) in Duchene muscular dystrophy using nuclear magnetic resonance spectroscopy. A comparison with normal controls is also made. Some of the groups like phenylalanine (-CH) , cysteine , serine are not found in DMD patients . These groups are found in healthy controls. A group Leuicine (-CH) was appeared in cases only . NMR spectroscopy is a powerful tool to detect the chemical groups of amino acids in serum.

Keywords : Chemical shift; Gyromagnetic ratio , Nuclear Magnetic Resonance; Immunoglobulin G ; Duchene muscular dystrophy .

1. INTRODUCTION

In the present work we intend to report our studies on macromolecule involved in Duchene muscular dystrophy using nuclear magnetic resonance (NMR) technique. Our main aim is throw light on the crucial mechanisms, which are responsible for transition from normal state to dystrophic state. Nuclear magnetic resonance (NMR) technique of spectroscopy branch is a next step of X-ray crystallographic studies. This method can provide high resolution structure of biological molecules. These macro molecules are proteins and nucleic acids and their complexes at atomic resolution. When a molecule is placed in a magnetic field its electrons are made to circulate and while circulating they generate secondary magnetic field. Circulation of electrons about the proton itself generate a field aligned in such a way that act at the proton it opposes the applied field. The field experienced by the proton is diminished and the proton is said to be shielded. Circulation of electrons about nearby nuclei generates a field that can either oppose or reinforce the applied field at the proton depending on the proton location. If the induced field opposes the applied field, the proton is shielded. If the induced field reinforces the applied field, then the field felt by the proton is de-shielded. Compared with a naked proton, a shielded proton requires a higher applied field strength to provide the particular effective field strength at which absorption occurs.

DOI: 10.14738/jbemi.11.99
Publication Date:15th February 2014
URL: http://dx.doi.org/10.14738/jbemi.11.99

Shielding thus shifts the absorption up field and de shielding shifts the absorption downfield. Such shifts in the NMR absorption, arising from shielding and de shielding by electrons are commonly called chemical shift ((δ)) and are measured in parts per million (ppm). The ^{1}H atom is the atom present in proteins that can be observed by NMR. Low natural abundance of ^{13}C atom can be used to some extent, and ^{13}C and ^{15}N atoms can be incorporate into the protein during biosynthesis. All the ^{1}H atoms of a protein can be observed, except those labile hydrogen atoms of –NH–, –NH2, –OH, and –SH– groups that are exchanging with hydrogen atoms in the aqueous solvent at rapid rates.

An NMR spectrum is a graph of the intensity of absorption (or emission) between frequencies. The spectrum of NMR generally appears in the low range of frequency, i.e., 10 to 800 MHz. Positions of the lines can be measured in ppm. This shift scale tells about the frequencies. It has given that frequency of NMR line is directly proportional to the magnetic field strength [1]. NMR spectroscopy is a powerful tool for both qualitative and quantitative analysis of organic compounds. There is a little use in clinical laboratory. The cost and complexity of the instrumentation is that NMR has not had sufficient quantitative sensitivity for most compounds of clinical interest. NMR spectra provide so many informations related to clinical aspects of the human system. The position of peaks determined by chemical shifts and spins – spin coupling constants, are characteristic of particular compounds and useful for quantitative analysis. The peak areas under some appropriate conditions are proportional to the number of resonating nuclei. This provides accurate quantitative analysis. Relaxation times and peak widths give informations about molecular dynamics and chemical kinetics .A single spectrum discloses the presence of any detectable compound. This technique may be used as a screening technique in selected situations NMR may also be used to screen for ingested toxins at high concentrations If a patient is alcoholic serum of the patient has high osmolality. We can eliminate problems of extractions recovers, contamination, or other artifacts by performing measurements directly on human serum.

2. BASIC THEORY OF NUCLEAR MAGNETIC RESONANCE SPECTROSCOPY

The nuclear magnetic moment is a quantum mechanical feature of a nucleus. NMR is based on the following principle. If a nucleus is well placed in a magnetic field which is static in nature, the nuclear spin will start to process around this applied field. This happens due to the fact that magnetic moment ( ) of the nucleus is related to the nuclear spin by the following relation.

The nuclear magnetic moment is a quantum mechanical feature of a nucleus. NMR is based on the following principle. If a nucleus is well placed in a magnetic field which is static in nature, the nuclear spin $\vec{I}$ will start to process around this applied field. This happens due to the fact that magnetic moment ($\vec{\mu}$) of the nucleus is related to the nuclear spin $\vec{I}$ by the following relation.

$$\vec{\mu} = \gamma\hbar\vec{I} \qquad (1)$$

We may see a precession called Larmor precession in the Figure 1.

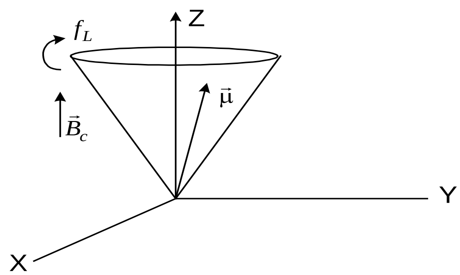

Figure 1 : Larmor precession

γ is called gyromagnetic ratio of the nucleus.

The frequency of this precession is called Larmor frequency and is given by the following relation

$$f_L = \frac{\nu}{2\pi} B_0 \qquad (2)$$

B_0 is magnitude of the magnetic field

This field is aligned with Z- axis and f_L is termed as Larmor frequency.

Each isotope has a well-known gyromagnetic ratio. $\gamma = 2\pi \times 42.58$ MHz /T (for protons)

Some informations have supplied regarding adiabatic change in magnetic field by [2] . If the change of direction of the magnetic field is sufficiently very slow, the axis of the precession cone of the magnetization vector follows the direction of the field. The angle of the cone will be unchanged.

If we consider the momentary rate of change of $\vec{B}$ as

$$\frac{d}{dt}\vec{B} = \vec{\Omega} \cap \vec{B} + \Omega_1 \times B \qquad (3)$$

The rate of change of $\vec{B}$ is expressed as the sum of the two components, perpendicular and parallel to $\vec{B}$. The quantities Ω and Ω_1 are dimensions of S^{-1} can be interpreted as Ω determines the angular velocity with which $\vec{B}$ changes its direction and Ω_1 determines the speed of change of $\vec{B}$. If the coordinate system is Cartesian in which z-axis follows $\vec{B}$ and maintains the direction. The motion of the magnetization in the rotating frame of reference is given below

$$\frac{d}{dt}M = \gamma M \times \left(B + \frac{\Omega}{\gamma}\right) \tag{4}$$

If we have no quadrupole interaction, the motion of the quantum mechanical spin moment $\vec{\mu}$ can be explained classically. We may add all these spin moment of an given ensemble of nuclei add up to a magnetization vector which is given here as

$$\vec{M} = \sum_k \vec{\mu}_k \tag{5}$$

$\vec{M}$ is called macroscopic magnetization. We can manipulate this magnetization vector in NMR experiment. Bloch [3] was the first scientist who described the equation of motion of this magnetization vector. Because it is composed of magnetic moment, it will experience a torque $\vec{M}\times\vec{B}$ on putting in a magnetic field $\vec{B}$.On the basis of this act we may conclude that as a result of this any magnetization which is de aligned with the magnetic field will presses around this field. The change in magnetization together with an extra relaxation contribution gives a Bloch equations which is given below

$$\frac{dM(t)}{dt} = \vec{M}(t)\times\vec{B}(t) - R\left(\vec{M}(t) - \vec{M}(0)\right) \tag{6}$$

Here R is tensor represents the relaxation mechanism.

We may write Bloch equation in three Cartesian coordinate along all the three coordinate axes respectively.

$$\frac{dM_Z(t)}{dt} = \gamma\left[M_x(t)B_y(t) - M_y(t)B_x(t)\right] - R_1\left[M_z(t) - M_0\right], \tag{7}$$

$$\frac{dM_x(t)}{dt} = \gamma\left[M_y(t)B_z(t) - M_z(t)B_y(t)\right] - R_2\left[M_x(t)\right], \tag{8}$$

$$\frac{dM_y(t)}{dt} = \gamma\left[M_z(t)B_x(t) - M_x(t)B_z(t)\right] - R_2\left[M_y(t)\right] \tag{9}$$

If we are dealing with pulsed NMR spectroscopy under the rotating frame for short pulse duration $\tau < 1/R_1$ or $1/R_2$ and if it is time independent B_1 and φ then Bloch equations became.

$$\frac{dM_z(t)}{dt} = \gamma\left[M_x(t)B_y{}^r - M_y(t)B_x{}^r\right] \tag{10}$$

$$\frac{dM_x(t)}{dt} = -\Omega M_y(t) - \gamma M_z(t)B_y \tag{11}$$

$$\frac{dM_y(t)}{dt} = \Omega M_x(t) + \gamma M_z(t)B_x{}^r \tag{12}$$

These equations can be written in matrix form

$$\frac{dM(t)}{dt} = \frac{d}{dt}\begin{bmatrix} M_x(t) \\ M_y(t) \\ M_z(t) \end{bmatrix} = \begin{bmatrix} 0 & -\Omega & -\gamma B_y{}^r \\ \Omega & 0 & \gamma B_x{}^r \\ \gamma B_y{}^r & -\gamma B_x{}^r & 0 \end{bmatrix} \tag{13}$$

and

$$M(\tau_p) = R_x(\phi) R_y(\theta) R_z(\alpha) M(0) \tag{14}$$

If we apply a radio frequency (RF) field. The total magnetic field is the sum of the static magnetic field $\vec{B}_0$ and the time varying magnetic field produced by the RF field $\vec{B}_{RF}(t)$:

$$\vec{B}(t) = \vec{B}_0 + \vec{B}_{RF}(t) \tag{15}$$

If RF is relatively small then

$$\vec{B}_{RF}(t) = \begin{bmatrix} B_1 \cos(\omega_{RF} t + \varphi) \\ B_1 \sin(\omega_{RF} t + \varphi) \\ 0 \end{bmatrix} \tag{16}$$

B_1 is the strength of the RF magnetic field and is directed perpendicular to the Z –axis, ω_{RF} is the frequency, φ is a phase offset of the field.

Bloch equation can be solved easily on the basis of this fact if we consider a coordinate frame rotating with the RF frequency, i.e., fixed to $\vec{B}_1$. We have already known about this static coordinate frame which is called laboratory frame and this rotating frame is called rotating frame of reference.

Under the influence of this rotating frame, the precession of the magnetic moment $\vec{\mu}$ of a nucleus is described by the following equation

$$\frac{\partial \vec{\mu}}{\partial t} = \gamma \vec{\mu} \times \left(\vec{B}_0 + \frac{\vec{\omega}_{RF}}{\gamma} \right) \tag{17}$$

This equation (17) shows that the effective magnetic field in the rotating frame of reference along the Z-axis is given by the following relation

$$\vec{B}_{eff} = B_0 + \frac{\vec{\omega}_{RF}}{\gamma} \tag{18}$$

The total magnetic field within this frame can be written as

$$\vec{B}(t) = \begin{bmatrix} B_1 \cos(\varphi) \\ B_1 \sin(\varphi) \\ B_0 - \omega_{RF/\gamma} \end{bmatrix} \tag{19}$$

If the RF frequency ω_{RF} is exactly equal to Larmor frequency ω_L, the Z-component of this total magnetic field in the rotating coordinate frame is equal to zero due to resonance condition given by equation (1) Now magnetization will process within the rotating frame around the direction of $\vec{B}_1$ with a frequency

$$f_1 = \frac{\gamma}{2\pi} B_1 \tag{20}$$

The magnitude of RF field is much smaller than the main magnetic field, f_1 is also the Larmor frequency. If we have applied B_0 is 1 T then f_1 will be equal to 42.58 MHz. Radio frequency (RF) is to be kept at same frequency. The amplitude of this field 1 mT. For a rotation of magnetization by a quarter of a full cycle (90^0 pulse), RF field needs to be 6 μs. We may say not only 90^0 pulse can be applied by the RF field, but more general value of angle of rotation β is given by the relation

$$\beta = 2\pi f_1 t_{RF} \tag{21}$$

This angle is called flip angle t_{RF} is the duration of the RF pulse. The phase offset φ between the rotating frame and the RF signal in equation (21) determine the axis around the rotation of $\vec{M}$ will occur. If a β pulse is giving a rotation around the x' -axis is denoted by $\beta_{x'}$ (flip angle of pulse). We shall consider here the action of a RF pulse on this magnetization as viewed in the rotating frame is presented in Fig. 2.

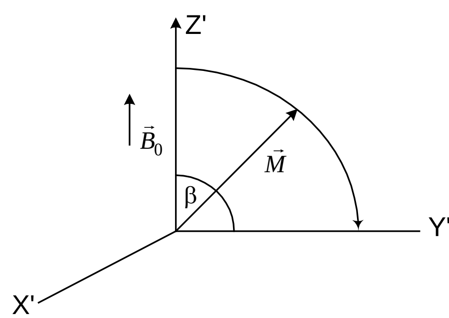

Figure 2: Rotation of magnetization with in the rotating frame of reference induced by a $\beta_{x'}$ pulse.

The magnetization, which was originally aligned with the z' axis of the rotating frame, now has changed into

$$\vec{M}(t) = M_0 \begin{bmatrix} 0 \\ \sin\beta \\ \cos\beta \end{bmatrix} \tag{22}$$

M_0 is original amplitude of this magnetization. This magnetization is stationary in the rotating coordinate frame, but in the laboratory frame, it is still processing with Larmor frequency.

Relaxation speed may be defined as linearly dependent on the difference of the actual magnetization and the equilibrium magnetization $\vec{M}(0)$. This will give exponentially decaying magnetization components.

If $\vec{B}_1$ is aligned with the z-axis, the relaxation tensor can be written as in the laboratory frame

$$R = M_0 \begin{bmatrix} 1/T_2 & 0 & 0 \\ 0 & 1/T_2 & 0 \\ 0 & 0 & 1/T_1 \end{bmatrix} \quad (23)$$

T_1 and T_2 are called longitudinal and transverse relaxation times respectively.

The physical background of the two relaxaton mechanisms is different. The longitudinal relaxation time is the spins need to exchange energy with the surroundings thermal reservoir or lattice. We may termed as spin –lattice relaxation time. The transverse relaxation time is the time in which spin dephase due to interactions with their neighbours and the presence of fast changing molecular fields. It is called spin – spin relaxation time.

Spin lattice relaxation time is calculated with the help of an equation which is given here as

$$\frac{dM_z(t)}{dt} = R_1\left[M_0 - M_z(t)\right] \quad (24)$$

Transverse relaxation time may be calculated by the help of eq. (a) and (b) of eq. (25) as

$$\frac{dM_x(t)}{dt} = R_2\left[M_x(t)\right] \quad (25a)$$

$$\frac{dM_y(t)}{dt} = R_2\left[M_y(t)\right] \quad (25b)$$

NMR spectroscopy can be used in protein dynamics and some of the calculations are shown here. The spectral density function $J(\omega)$ may be related to the relaxation rates.

The probability function of finding motions at a given angular frequency ω can be described by the special density function as

$$J(\omega) = \frac{2\tau_c}{1+(\omega\tau_c)^2} \quad (26)$$

The relaxation rates which are associated with the protein dynamics given below.

$$R_1 = 3AJ(\omega_N) + AJ(\omega_H - \omega_N) + 6AJ(\omega_H + \omega_N) + BJ(\omega_N) \quad (27)$$

$$R_2 = 2AJ(0) + \frac{3A}{2}J(\omega_N) + \frac{A}{2}J(\omega_H - \omega_N) + 3AJ(\omega_H) + 3AJ(\omega_H - \omega_N) + \frac{2B}{3}J(0) + \frac{B}{2}J(\omega_N) \quad (28)$$

$$\sigma = -AJ(\omega_H - \omega_N) + 6AJ(\omega_H + \omega_N) \quad (29)$$

Coefficient A and B are

$$A = \left(\frac{\mu_0}{4\pi}\right)^2 \frac{\gamma_N{}^2 \gamma_H{}^2 \hbar^2}{4r^6{}_{NH}}, \tag{30}$$

$$B = \frac{\Delta\sigma^2{}_N B^2{}_0 \gamma^2{}_N}{3} \tag{31}$$

Nuclear Overhauser effect (NOE) may be calculated and it is given here

$$NOE = 1 + \frac{\sigma}{R_1} . \frac{\gamma_H}{\gamma_N} \tag{32}$$

μ_0 is the permeability of the vacuum, γ_N is gyromagnetic ratio of the ^{15}N nucleus, γ_H is gyromagnetic ratio of the ^1H nucleus, $\hbar$ is plank's constant , r_{NH} is $^{15}N - {}^1H$ inter-nuclear distance, $\Delta\sigma_N$ is chemical shift of anisotropy of the ^{15}N nucleus, B_0 is static magnetic field strength

It has been well established that the use of NMR spectroscopy in the field of biology is vast and very much fruitful in studying the structure of protein in detail. Small amount of the sample is needed for study. Due to this fact we have used NMR technique and applied it to study the structure of human immunoglobulin G (IgG). Immunoglobulins are called as globular proteins.

The proton is most widely used nucleus for applications of NMR spectroscopy in clinical investigations. The wide spread biological applications of NMR can not be covered in small detailed work. We may use NMR to detect the correct diagnosis of diseases.

The nuclear spin is associated with a magnetic moment which is required for obtaining nuclear magnetic resonance. This also defines the basic resonance frequency. It has been seen that at 14.1 Tesla there is a resonance frequency of 600 MHz for ^1H and 150 MHz for ^{13}C. Every spin in a given molecule produces a nuclear magnetic resonance line. The resonant frequency at exact position depends on the chemical environment of each spin. The NMR spectrum of protein shows NMR signals with slightly different frequencies. The difference in frequencies is called chemical shift. The assigning of these chemical shifts of all the atoms of the molecule is a step in determination of structure of a molecule by NMR. Experimental parameters may be measured after the assigning of NMR signals. Structural informations derived from NMR spectra are completely based on nuclear Over hauser effect (NOE). This effect is due to dipolar interactions between different nuclei. The intensity of NOE is given by the following relation

$$NOE \propto \frac{1}{(r)^6} f(\tau_c) \tag{33}$$

r is called the inter nuclear distance

$f(\tau_c)$ is called the correlation functions.

This function describes the modulation of the dipole – dipole coupling by stochastic rate process, with an effective correlation time τ_c.

NOEs may be observed between protons which are separated by less than 5 -6 Å. A new factor which is called J coupling constant are mediated through chemical bonds may provide some information about dihedral angles. These can define peptide backbone and side chain conformations. Residual dipolar coupling (RDC) and Cross correlation relaxation effect (CCR) have been shown to provide distance independent projection angles for bond vectors. These are N-H and C^{α} & H^{α} bonds in proteins. The residual dipolar couplings may be measured in anisotropic solution also.

It has been reported in the literature the 3-D structures can be obtained for proteins up to 50 kDa molecular weight. Pelton et.al. [4] have used this technique and NMR spectra can be recorded for molecules well above 100 kDa. The use and application of biomolecular NMR in structural biology are introduced. Biomolecular NMR may provide very important information in solution for structure determination . This sophisticated technique of spectroscopy can provide information about the conformational or chemical exchange, internal mobility and dynamics at time scales. The averaging of side chain conformation may be estimated and the populations of different conformations can be determined. NMR may provide information on the location of secondary structural elements within the protein sequence.

3. REVIEW OF THE LITERATURE

The application of NMR in the study of biological molecules has become an important ingredient. This technique was first applied to investigate the bulk material by Purcell [5] and Bloch et. al. [3]. Pioneering work was carried out by Jardetzky et.al . [6], Kowalsky et.al. [7] and McDonald. et.al. [8] in the field of relevant biomolecules. Proteins are the most studied by biopolymers. The protein spectra are very complex and simulation by mixing of amino acids does not produce the replica of the observed spectra in them as the intricate folding at the polypeptide chain makes major changes in both chemical shift as well as relaxation effect (line broadening).

Important structural information are revealed by NMR spectra, which are characterized by parameters like peak position, width, intensity and multiplicity of its line. One can find the different proton groups present in the molecule by the number of lines present in NMR of a particular molecule. The integrated area of a line gives the relative number of protons in each groups and also information about the environment of the molecule. The hyperfine splitting reveals the interaction between a particular nucleus and its neighbors. The line width increases with the size and rigidity of the molecule. However in a large molecule there is an overlapping of peaks which can be overcome by increasing the frequency of the spectrometer. The NMR spectra arise due to the absorption of energy during transition from low (more populous) to the higher (less populous) energy state in a nucleus. The detectable absorption is characteristics of the environment of the nucleus. With the variation of frequency the resonance will be the function of the local molecular environment and of the magnetic field in which the nucleus find itself.

Improvement in NMR technology is one of the most recent method, applied to the diagnosis of human diseases [9-12]. Chalovich et.al. have given a statement that the nuclei common in tissues ^{1}H was used for NMR imaging of the organs of human subjects and to analysis the composition of human serum of the various applications of NMR for medical purpose, the method is most sensitive for analysis of serum. Bradbury et.al. [13] has also applied NMR in the investigation of structure of histones Leeet.al. [14] and Chapman et.al.[15] have studied molecular basis of interaction of histones with nucleic acid, analysis of flexibility gradient in phospholipids membranes and in understanding the biological importance of bound water.

Wüthrich [16] has supplied informations related to NMR studies of structure and function of biological macromolecule. NMR spectroscopy is unique among the techniques available in science for 3-dimentional structure determination of proteins and nucleic acids. NMR can be done in solution. Body fluids such as blood, stomach liquid and saliva and protein solutions where these molecules perform their physiological functions. Study of the molecular structures in solution is to much relevant and desirable. Solution conditions such as the temperature, pH and salt concentration can be adjusted so as to closely mimic a given fluid (physiological fluid). Solutions can be changed into non-physiological conditions such as protein denaturation. NMR investigates the dynamic features of the molecular structure, as well as studies of structural, thermodynamic and kinetic features of interactions between proteins other solution components. These may be other macromolecules or low molecular weight ligands.

Some of the major improvements in NMR hardware and methodology have been made by the scientists. Due to these improvements the use of NMR for the characterization of structure and dynamics of biological molecules in solution has become very important. These improvements are still into consideration and on going and are designed to overcome the main problem with NMR of biomolecules, namely signal to noise ratio and spectral overlap. Biomolecular NMR spectroscopy may give information about conformational dynamics and exchange processes of biomolecule at time scales ranging from 10^{-8} seconds (picoseconds to seconds). This technique is also effective in determining ligand binding and mapping interaction surfaces of protein /ligand complexes. Proteins are orders of magnitudes larger than the small organic molecule. NMR spectroscopy is applied to study of proteins because increased number of each element present in the molecule.

Kurosu et al. [17] have studied synthetic macromolecules with the help of NMR. NMR has been the most suitable technique to characterize and to investigate the correlation between the structure and physical properties. Prior [18] has studied NMR in living systems such as eye, tissue of heart muscle, reproductive tissue, brain, liver, bone marrow, etc. The author has reported that the linewidth of lipid and water differed significantly between groups.

Jardetzky [19] has reported the finding on determination of macronuclear structure and dynamics by using NMR. He pointed out the basic problem of interpreting spectroscopic data in structural terms from the fact that measured parameters represent motional as well as ensemble averages. If we have a non-rigid system, a unique correlation between measured spectroscopic parameters and structural parameters such as interatomic distances and coordinates does not exist. A straightforward calculation of the structure is not possible. NMR parameters are the function of distances, motions, frequencies and amplitudes. These parameters can supply the well-defined relationship regarding the interatomic distances. Hounsell [20] has studied carbohydrates, lipids and membranes with the help of NMR. There is a study on cerebrospinal fluid of different diseases and a clear cut differentiation was found in the atomic and molecular level in terms of chemical shifts. Simpson [21] has studied and reported the findings on proteins and nucleic acids. The assignment of small proteins is regular system nowadays. The specific amino acid labeling can still be of use for assisting peak identification. Consanni. et al. [22] have studied nuclear magnetic resonance and chemometrics to access geographic origin and quality of traditional food products. They have reported their view for NMR and chemometrics, which were reviewed and applied to food quality and geographical origin determination.

Adam. et al. [23] have applied carbon-13 NMR to study the proteins and glycoproteins. They have also studied globular proteins and recorded NMR spectra at 15.18 MHz. Some overlap between the aliphatic region and amino acid residues has been obtained. NMR can be used as a tool to study the bio-molecules in the field of biochemistry. Talebpouret al. [24] have applied this technique to identify and determine the caffeine and theophylline in human serum. They have reported their findings for the caffeine peaks which were obtained at 2.75, 2.93 and 3.40 ppm. Theophylline peaks were found at 2.77 and 2.97 ppm. Wishrat [25] has studied NMR technique for the determination of proteins with the development of drug discovery. It has been noticed that the first crude protein structure was determined in the year 1980. NMR can play a role in the area of protein based drug discovery. It gives the structural information along with the dynamics of the protein. Newman et.al.[26] have applied nuclear magnetic resonance spectroscopy to the forearm muscle in DMD and found that the phosphorous spectrum was abnormal in the ratios of phospho-creatine to adenosine triphosphate and to inorganic phosphorus were reduced .They have also reported that the concentration of phosphocreatine in muscles was appreciable reduced . Sharma et.al.[27] have studied skeletal muscle metabolism in Duchenne muscular dystrophy and reported that decrease in levels of glucose may be attributed to the reduction in the concentrations of gluconeogenic substances or membrane abnormalities . A decrease in the concentration of lactate in the muscle of DMD patients may be due to the reduction in anaerobic glycolytic activity or lower substrate concentration.

Matsumura et.al.[28]have studied DMD carrires with the help of magnetic resonance imaging and p ersumed that degenerative muscular changes accompanied by interstitial edema responsible for this disease . They have given a conclusion that NMR is useful for study the dynamic state of water in normal and pathological skeletal muscles . Zochodne et.al .[29] have studied fore arm P-31 nuclear magnetic resonance spectroscopy in oculopharyngeal muscular dystrophy and found that this dystrophy is a more wide spread disorder of striated muscle than clinically appreciated . Sharma et.al.[30] have studied biochemical characterization of muscle tissue of girdle muscular dystrophy with 1H and 13C NMR spectroscopy . They have found that a significant reduction in the concentration of choline in the patients and healthy controls .Lower concentration of choline may be out come of decreased rate of membrane turn over in the patients .Barbiroli et.al [31] have studied 31P NMR spectroscopy of skeletal muscle in Becker dystrophy and DMD/BMD carriers . They have found that in the working muscle of BMD patients and female DMD/BMD carriers a defect of phosphate metabolism. It reflects a deficit of energy metabolism.

Donaldet.al.[32] have studied 31P NMR in DMD to measure high energy phosphate compounds and phosphorylated diesters in resting gastrocemius muscle . They have shown a progressive metabolism deterioration in this disease. Griffin et.al. [33] have studied metabolic profiling of genetic disorders in dystrophic tissue with the help of NMR spectroscopy . They have reported that many metabolic pathways are perturbed in dystrophic tissue . Sharma et.al [32] have made analysis on the basis of NMR spectroscopy and given a statement related to ex vivo and in vivo NMR spectral peak observations in different diseases .This can support the reliability of clinical applications using in vivo localized 1H NMR spectroscopy peaks to determine the biochemical cause of disease .Šuput et.al.[35] have used magnetic resonance imaging technique to muscular dystrophies and neuropathies . They have reported that musculature may be replaced gradually by adipose tissue. Authors disclose clear differences in the degeneration of particular groups of muscles. Cady et.al [36] have studied this spectroscopy to muscle metabolism and reported that the clinical use of NMR is very useful in the study of muscular dystrophy . They have mentioned in the article as the mean resting metabolic levels and pH determined by 31P NMR and indicates significant differences between values for PCr, Pi, PCr/Pi and PCr/ATP compared with normals. Chance et. al. [37] has applied this technique to normal and diseased muscle. They have used phosphorous magnetic resonance spectroscopy ,which affords and innovative approach to study of the oxidative enzyme content of normal and diseased muscles .Michael et.al.[38] have used Carbon13 NMR spectroscopy to study normal and abnormal muscles and reported that13C NMR of isopentane – extracted muscles have shown a clear cut differentiation of normal from diseased muscles and within diseased muscle, grading of the severity of the disease .Schreiber et.al [39] have used magnetic resonance imaging to muscular dystrophy in children .They have given a statement on the basis of scans of the five muscles groups, i.e. neck , shoulder gridle, pelvis gridle , thigh and calf . They demarcated the involved muscles. The severity of the disease estimated by the degree of muscle involvement. Kaisr et. al [40] have used 31P NMR to study normal and diseased muscle. They have pointed out that abnormal muscles showed characteristic changes in phosphorous spectrum , when compared with normal muscles .Bottomley et.al .[41] have used proton magnetic resonance spectroscopy and given a statement that this spectroscopy can be used to image and noninvasively quantify total creatine in human muscle. Role of altered creatine metabolism in muscle disease can be studied with this spectroscopy .Garrood et.al. [42] have used NMR imaging and reported that referenced signal intensity measurement may be used to quantify difference between dystrophic and normal muscle without T(1) mapping.Ogino et.al. [43] have studied serial water changes in human skeletal muscles .

They have measured the changes in signal intensity in both calf muscles after walking race exercise .The time intensity curves were also used to draw a clearance curve for each muscle group after exercise. Srivastava. et.al.[44] have studied high resolution NMR based analysis of serum lipids in Duchenne muscular dystrophy patients and its possible diagnostic significance and reported that concentration of triglycerides, phospholipids , free cholesterol esters and and total cholesterol was significantly higher in DMD patients as compared to healthy patients . They have also given a statement that no significant quantitative difference was observed in the serum lipid constituents of positive and negative gene detection in cases of DMD. It may be useful to provide the possibility of the diagnostic importance for DMD, especially in cases where genetic analysis failed to give the correct diagnosis. Sarpel et.al.[45] have studied erythrocytes in muscular dystrophy with the help of 31P NMR and measured the inorganic –phosphate fraction contained the highest average phosphate concentration over sixteen hour period .This result contributed to the difference in the total phosphate between two groups. Bock, J.L [46] have studied serum by high field proton magnetic resonance spectroscopy and suggested that the nondestructive nature of NMR, which is the basis of its in vivo applicability .We can also use this facility in the vitro analysis. We can eliminate problems of extraction recovery, contamination, or other artifacts .Forbes .et .al. [47] have used this technique to study skeletal muscle of ambulant children with Duchenne muscular dystrophy and stated that the MR protocol implemented in the study achieved highly reproducible measures of lower extremity muscles in ambulant boys of DMD.

4. MATERIALS AND METHODS

The blood samples of DMD patients were collected from the Department of Neurology, Safdarjang Hospital, New Delhi. Twenty milliliters freshly drawn blood from each patient was collected in clean and dry test tube without any anti- coagulant. The test tube was kept for 45 minutes at room temperature ($22 \pm 2^{0}C$) for the formation of clot. Sera of different patients were separated by centrifugation at 1500 r.p.m. upto 15 minutes and were collected in screw capped test tubes. IgG sample were prepared on protein A –Sepharose [48]. The IgG binding properties of protein A, make affinity chromatography with protein A -- sepharose CL- 4B a very simple method for preparing IgG. 1.5 g protein -A sepharose CL-4B was swollen in 10 ml phosphate buffered saline (PBS) for 1 hour at room temperature and then packed into a small chromatography column. 10 ml human serum was diluted with an equal volume of PBS. The serum was filtered through the column at a flow rate of 30 ml/h. Washing was done through unbound protein with PBS. Until no more protein left the column (the protein was monitored with a UV flow cell). The bound IgG was eluted with glycine- HCL buffer having a pH value of 2.8. The pH of the purified IgG solution was titrated to near neutrality with NaOH.and dialysed against PBS. The column was regenerated by washing with 2 column bed volume of PBS. The column was stored at 4°C. The protein A content of the swollen gel is 2 mg /ml and the binding capacity for human IgG is approximately 25 mg /ml of packed gel.As the binding of protein A to IgG involves tyrosine residues on the protein A glycosyl tyrosine (0.1M in 2 % (NaCl) can be used to elute the IgG rather than the the glysine – HCl buffer. The NMR spectra of the IgG samples extracted from normal person and Duchenne muscular dystrophic patients were recorded on Av Bruker 500 MHz NMR Spectrophotometer (Fig. 3) in central NMR facilities I.I.T. New Delhi, India.

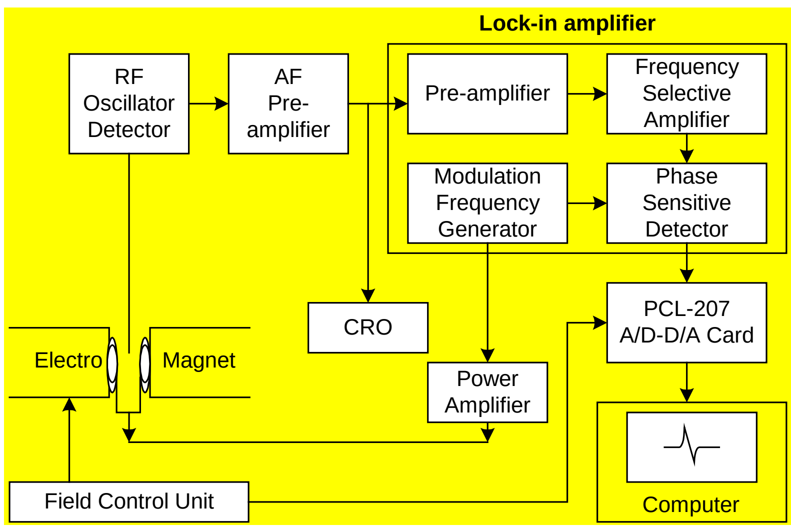

Figure 3: Block diagram of Nuclear Magnetic Resonance Spectrometer

5. RESULTS

We have applied NMR spectroscopy to IgG molecule of DMD children and findings are reported in the table form. We have compared our data with the normal healthy controls. Typical NMR spectra of normal and DMD patient are given in Fig.4 and Fig.5

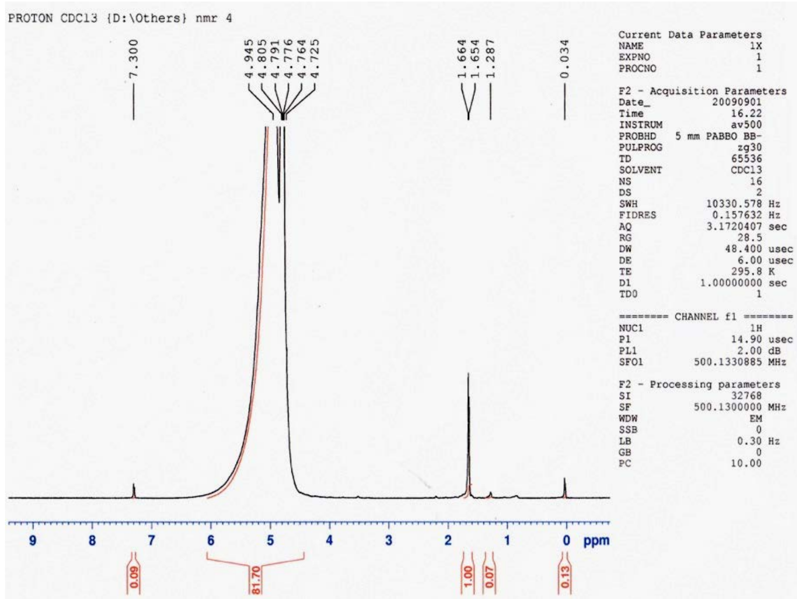

Figure 4: Typical NMR spectra of normal sample

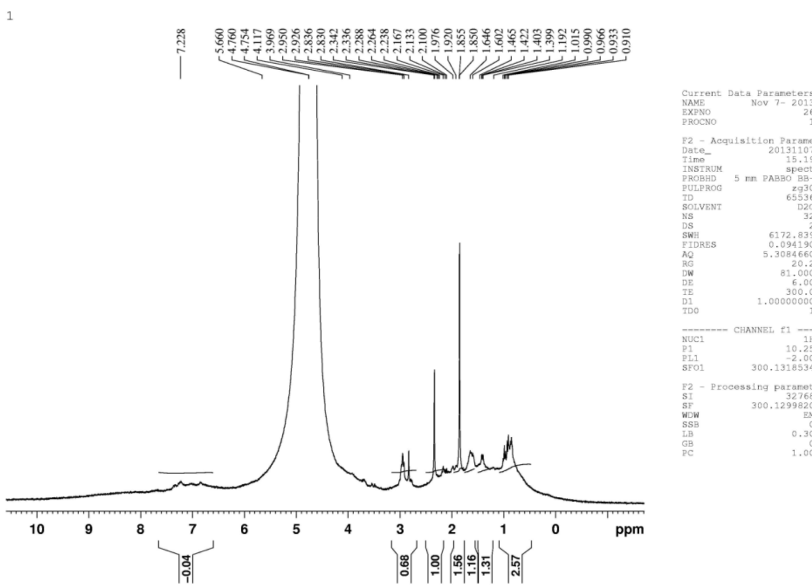

Figure 5: Typical NMR spectra of DMD sample

Table 1. Comparison between different probable groups of the amino acids of IgG with peak intensities in DMD and Controls

S. No.	Type of sample	Peak position	Chemical shift □ ppm	Probable group	Standard values	D_2O peak
1	N	1 2	0.87 1.34	Isoleucine, □CH_3 Alanine, □CH	0.89 1.36	4.73

		3 4 5 6	2.05 3.24 4.14 4.65	Glutamic acid, □-CH Cystine, □□□ C Isoleucine □-CH Phenylalanine □-CH	2.09 3.28 4.14 4.65	
2	N	1 2 3 4 5 6	0.88 1.28 2.04 3.25 4.61 4.64	Isoleucine, □-CH_3 Alanine, □-CH Glutamic acid, □-CH Histidine, □-CH Tyrosine, □-CH Phenylalanine, □-CH	0.89 1.36 2.09 3.26 4.62 4.66	4.73
3	N	1 2 3 4 5 6	0.87 1.28 2.03 3.22 4.12 5.31	Isoleucine, □-CH_3 Isoleucine, □-CH_2 Glutamic acid, □-CH Phenylalanine, □-CH Valine, □-CH	0.89 1.22 2.09 3.22 4.13	4.73
4	N	1 2 3 4 5 6	0.87 1.20 1.34 2.12 3.66 5.90	Isoleucine, □-CH_3 Isoleucine, □-CH_2 Alanine, □-CH Gln, □-CH Glycine, □-CH	0.89 1.22 1.36 2.13 3.64	4.77
5	N	1 2 3 4 5 6	0.88 1.21 2.09 3.22 3.66 4.14	Isoleucine, □-CH_3 Isoleucine, □□ CH Glutamic acid, □-CH Phenylalanine, □-CH Glycine, □-CH Glycine □-CH	0.89 1.22 2.09 3.22 3.64 4.14	4.78
6	N	1 2 3 4 5 6	3.75 3.93 4.32 4.74 5.14 -	Serine, □-CH Serine, □-CH Methionine, □-CH Cystine, □-CH	3.79 3.95 4.32 4.74	4.70
7	N	1 2 3 4 5 6	0.87 1.22 1.39 3.24 4.33 4.62	Isoleucine□□-CH_3 Isoleucine□□-CH_2 Alanine Cystine Alanine Phenylalanine	0.89 1.22 1.39 3.28 4.35 4.66	4.70
8	N	1 2 3 4 5 6	0.87 1.22 1.39 3.24 4.33 4.62	Isoleucine Isoleucine Cystine Phenylalanine Tyrosine	0.95,0.77 1.48,1.22 3.28 4.58 4.62 ----	4.66
9		1 2	0.79 1.25	Isoleucine Isoleucine	0.89 1.48,1.22	4.67

	N	3 4 5 6	3.27 4.56 4.62 4.83	Alanine Cystine Glycine Tyrosine	1.36 3.28 4.14 4.62	
10	N	1 2 3 4 5 6	0.83 1.23 3.22 4.29 4.44 4.48	Isoleucine Isoleucine Cystine Serine Tyrocine Cystine	0.89 1.48, 1.22 3.27 4.52 4.61 4.67	4.73
12	DMD	1 2 3 4 5 6	0.68 1.00 1. 16 1.31 1.56 2.57	Isoleucine, -CH_3 Isoleucine, -CH_3 Isoleucine, -CH_2 Alanine, -CH Leucine, -CH Asp, -CH	0.89 0.95 1.19 1.36 1.54 2.62	4.75
13	DMD	1 2 3 4 5 6	0. 34 0.50 1.00 1.13 1.50 2.22	Isoleucine, -CH_3 Isoleucine, -CH_2 Leucine, -CH Proline, -CH	0.95 1.22 1.50 2.22	4.75
14	DMD	1 2 3 4 5 6	0.54 1.00 1.02 1.54 1.72 1.74 3.64	Isoleucine, 3 Valine , 3 Leucine, C Leucine, CH Leucine, CH Proline, 2 CH	0.95 0.97 1.54 1.75 1.75 3.65	4.76
15	DMD	1 2 3 4 5 6	0.14 0.16 0.29 1.00 1.60 1.37 2.09	----- --- --- Isoleucine 3 Leucine, CH Analine, CH Glu CH	0.95 1.65 1.39 2.09	4.70
16	DMD	1 2 3 4 5 6	0.66 0.91 1.00 1.36 1.50 1.50 1.68 3.06 4.42	- Valine , 3 Isoleucine, -CH_3 Alanine , -CH Leucine , -CH - - Leucine , -CH Tyrosine , -CH Proline, -CH	-- 0.91 0.95 1.39 1.50 - - 1.75 3.08 4.44	4.75

According to data available with the present study we are giving some of the findings related to DMD patients . A group phenylalanine (β-CH) is completely absent in all DMD cases. We did not find any trace of this group in normal healthy controls .We also did not find another group called Leucine (β-CH and γ- CH) in normal controls .This group is found in DMD patients .Proline (β-CH)is present in two cases of DMD only .This group is also absent in all normal controls . We have also not found Cystine and Serine groups in DMD patients.

6. DISCUSSION

A magnificent use of NMR lies in fact that, because of the chemical shift, amino acids can be identified and isolated in the spectra of protein. It is well known in NMR theory that the motion of any type such as rotatory and translatory reduces the width of the resonance line .Due to this property motional narrowing feature starts and high resolution NMR is required. Proton magnetic resonance spectra of twenty amino acids and some representative di and tri peptide were studied by Mandel [49]. Vitolis et.al[50] have studied NMR spectrum of a serum sample shows both sharp narrow peaks from small molecule metabolites and broad peaks from proteins and lipids .The analysis of of spectrum of NMR for blood serum requires dealing with the effects of proteins and other large molecules.

NMR spectroscopy is the technique of spectroscopy that can provide detailed structural information about macromolecules at atomic resolution. Many scientists have been characterized small molecules by using empirical rules associated with the study of chemical shift regarding the conformation of the structure of the molecule.It has been seen that most of the amino acid spectra can be understood on the basis of first order effects. The chemical shift is larger than the spin –spin coupling.In the study of amino acids while the chemical shift is not large compared to the spin –spin coupling. We can compare the chemical shift and spin –spin interaction in this situation.If we have a situation that lies between these two experiments there are many amino acids the spectrum may have first and second order both. If we apply a large field to the system and we find a situation for the chemical shift, which is proportional to the field strength and kept spin –spin coupling as constant. Calculations based on chemical shifts are very useful in the structure of determination of globular proteins such as IgG.

Burton [51] has studied the structure and function of immunoglobulin G and reported some of the interesting applications of NMR to study this molecule. An antibody is a protein synthesized by an organism in response to invasion of the organism by a foreign substance termed as antigen. IgG found as principal antibody in serum. It has a molecular weight of about 150,000 and a domain structure is shown in Figure 6.

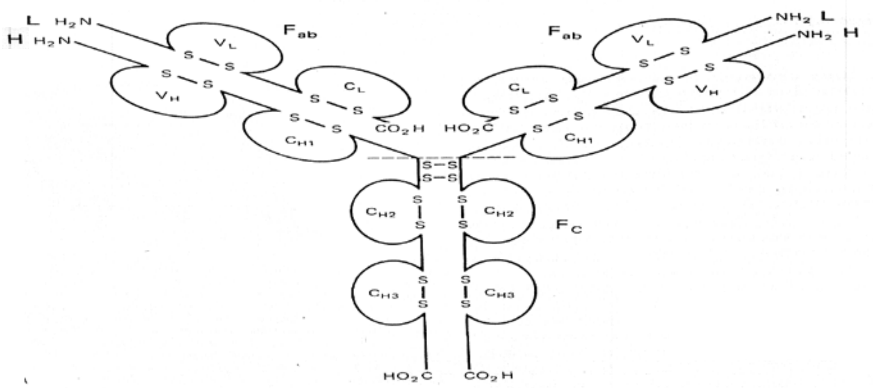

(A)

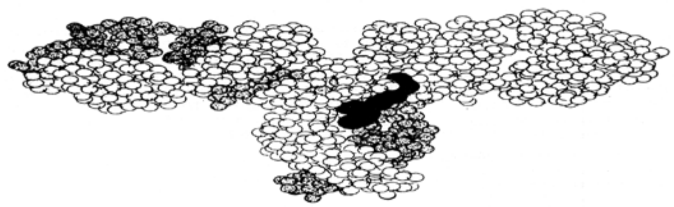

(B)

Figure 6: (A) Schematic diagram of a typical IgG structure; (B) Space filling model determined crystallographically

Mayer et al. [52] showed that IgG molecule can be cleaved into a number of proteolytic fragments. Antigen and complement bindings sites are also shown. If the antigen is not present, the complement site can be neglected. However, on the formation of a particular specifies antigen-antibody complexes, the first protein of the complement sequences binds to this site. This leads to activation of other proteins in the sequence and eventual destruction of the antigen.

It has been reported in the literature that IgG possess two equivalent tight Gd(III) sites located in the CH_3 domains of the Fc-region. Very much low affinity Gd(III) sites were also found on the FaS region. Experimental conditions may be adjusted such that IgG and the fragment Fc and pFc effects from the same two Gd(III) sites. They form a family of Gd(III) tight binding macromolecules of decreasing molecular weight. IgG has 150,000, Fc has 50,000 and pFc' has 25,000.

There is an internal motion found in the Fc portion of IgG. A considerable amount of motional freedom at Fc position was also found. A flexible rigid transition in the IgG molecule as the trigger for complement activation was also pointed out by Huber et al. [53].

Boyd et al. [54] have studied the mobility of protein on the basis of high resolution protein NMR of Fc and pFc' fragments. The spectra of such fragments appear resolved compared to the spectra of other proteins of similar molecular weight.

Cohn et al. [55] have studied the observations of amino acid side chains in proteins using this sophisticated technique of spectroscopy and reported in the research article regarding the side chain groups such as Glu, Asp, Lys, Arg, Met, Thr, Leu and others act as intrinsic non-disturbing probes of their local electronic microenvironment in a protein.Some of the authors [56-58] have studied the structure of proteins with the help of NMR spectroscopy in detail. They have found each proton resonance appears along the chemical shift axis in the expected fashion. The multiplets due to spin coupling appear only on the perpendicular axis.

If an amino acid residue in a protein is converted from a solvated state in a random coil polypeptide chain to buried inside the interior of a globular protein the chemical shift depends on the variation of magnetic susceptibility. Glick, et al. [59] have made their statements on amino acid residues and provide an interesting result such as chemical shift is directly proportional to the volume diamagnetic susceptibility K.

The NMR spectra of small globular proteins are very crowdy in nature. There is no evidence of unequivocal observations of Ser β-methylene proton resonance. Moore et al. [60] have studied and found that the assignments of the methyl-group resonance of Thr-47 and Thr-89 for ferricytochrome C and ferrocytochrome C.

Some of the authors Spero et.al. [61] and Kuszewski et.al. [62]have used chemical shift to obtain structural information regarding the correlation between chemical shifts and backbone torsion angles. It has been pointed out that different structures of proteins such as secondary, tertiary and quaternary have been successfully studied in solution and solid form and calculated with the help of chemical shift by various research scientists [63-70]. NMR chemical shifts are the best parameters and can be used in the structure elucidation of larger molecules. The assignment of backbone chemical shifts is necessary to determine the structure of protein.

Satoshi et al. [71] have studied proton nuclear magnetic resonance of human immunoglobulin G1 and its fragments. They have pointed out some information regarding the structure of hinge region and effects of a hinge region deletion on internal flexibility. Koichi et al. [72] have studied structural basis of the interaction between IgG and fcy receptors1. The studies on NMR spectroscopy show that Fcy RII binds to a negatively charged area of the CH_2 domain, corresponding to the lower hinge region. The binding of Fcy RIII onto one of the two related sites on the Fc induces a conformational change in the outer side.

Brab et al. [73] have studied NMR analysis on immunoglobulin G and glycenes and they have provided their fruitful results as glycan does not directly engage the cell surface receptors. The termini of both glycan brachs are highly dynamic and experience considerable motion in addition to tumbling of the Fc molecule.

The three dimensional structure of globular protein fluctuates incessantly and the fluctuation is closely related to the function of the protein. Nicholson et al. [74] have studied the dynamics of methyl groups in proteins.

Zilagyi et al. [75] have identified a correlation between αH chemical shifts and the helical and β-sheet structures. If the other effects are not present, helical conformation produces upfield shifts while β-structures shift the α proton downfield. Pasture et al. [76] have studied the secondary structure of proteins and Oldfield [77] studied three dimensional structure of proteins in terms of chemical shifts.

Jardetzky et.al. [78] have studied the protein spectra of amino acids and indicated these chemical shift are independent of concentration. Chemical shift mean a change in the chemical shift from that of the free amino acid. The real use high resolution NMR lies in the fact that because of the chemical shift specifies amino acids, which can be nicely and easily isolated in the spectra of protein. If we increase our understanding of the relationship between the chemical shifts and structure of the proteins or globular proteins such as immunoglobulin G molecule, we will be able to improve the accuracy of measurement and structure determination.

Proteins play a major role in the billions of process which occur in the body. It includes the development of muscles, skin, digestion of food, growth of cells and the germination of human emotions. These cells have a tendency to produce proteins continuously. We are not able to understand how these complex molecules exactly work.

Not only the chemical composition of the proteins but also the spatial structure of proteins is important for the performance of their functions. The way in which they fold and unfold in 3-D space help in determining the function of the molecules. It will be very difficult to understand the function of the molecules without detailed knowledge about their structure, spatial structure study is necessary now a days. NMR may help in the study of the determination of the structure of proteins. This technique can detect and quantify folding and conformation changes in proteins, while simultaneously providing detail structure information. If we use NMR spectroscopy in different diseases the NMR spectral peak observations can support the reliability of clinical applications. These peaks can determine the biochemical cause of the disease . However , peak identification ,peak intensities ,peak analysis of the given sample is a big support for the research scientists and clinicians.

7. CONCLUSION

The observed chemical shift in water peak in all the cases may be due to pathological conditions. The presence of the paramagnetic ions and the overlapping of protons from the changed line width. We have found peaks in all the spectra recorded on NMR due to the formation of some active centre's such as paramagnetic ions. The comparison of the diseased sample spectra with the normal's reveal some characteristics of the disease.

It is possible to identify the nature of the pathological disorder by looking at the NMR spectrum of patient's blood (immunoglobulin G molecule). It has been found that the peak intensities, line shapes and chemical shift were different. These basic properties suggest that there are perturbations present which vary from sample to sample. NMR spectra are interpretable only if the hydrogen atoms have unique chemical shifts . Considerable overlap of resonance occurs if there are too much resonances in any area of NMR spectrum . NMR also gives detailed information about the flexibility of the protein structure in solution[79] .The chemical shift suggests a transfer of electrons in enzymes and proteins in DMD. The dipolar anisotropy of unpaired electron causes a shift in line position. Sometimes delocalization is also coupled. We have found in the present study that the groups related to Phenylalanine, cysteine and serine were completely absent in all the DMD cases.

ACKNOWLEDGEMENT

The authors are thankful to Dr. P. K. Saxena, Principal, D.A.V. (P.G.) College, Muzaffarnagar for providing the facility of doing work. We are also thankful to Professor D. C. Jain, Head of the Department of Neurology, Safdarganj Hospital, New Delhi, for arranging the blood samples of the diseased and healthy controls. We are grateful to Dr. Manju Chauhan, Head, Department of Biosciences, D.A.V. (P.G.) College, Muzaffarnagar, for providing the facility of purification of IgG. Authors are thankful to Mr.Deepak Singh, Central NMR facilities, I.I.T. Roorkee for assistance in conducting experimental work.

REFERENCES

[1]. Keeler, J, *Understanding NMR Spectroscopy*, 2nd Edition, 2010, John Wiley & Sons Ltd,: p.5-21.

[2]. Hennel, J. W. and J. Klinowski, *Fundamental of Nuclear Magnetic Resonance, Longman Scientific & Technical*,1993 : p. 115.

[3]. Bloch, F, W.W. Hansen, and M. PackKard, *The Nuclear Induction Experiment. Physical Review*, 1946. 70 (7-8) : p. 474-485.

[4]. Pelton, J. T. and L. R. McLean, *Review Spectroscopic Methods for Analysis of Protein Secondary Structure.* Analytical Biochemistry, 2000. 277 : p. 167- 176

[5]. Purcell, E. M. *Resonance Absorption by Nuclear Magnetic Moment in a Solid*. Physical Review, 1946. 69 : P. 37.

[6]. Jardetzky, O., and N. G. Jardetzky, Application of Nuclear Magnetic Resonance Spectroscopy to Study of Macromolecules. Ann. Rev. Biochem, 1971. 40: p. 605 -674.

[7]. Kowalsky, A., and N. Cohn, *Applications of Nuclear Magnetic Resonance in Biochemistry*. Ann. Rev. Biochem, 1964. 33 : p. 481-518.

[8]. McDonald, C. E., and W. D. *Phillips, Fine Structure of Proteins and Nucleic Acids (Biological macromolecule series 4)*, G. D. Fasman, and Tunasheff, Editors , Marcel Dekker, 1970 : p. 1.

[9]. Edward, R. H. T., M. Joan. Davvson, D. R., Wilkie, R. E. Gorden, and D. Shaw, *Clinical use of Nuclear Magnetic Resonance in the investigation of Myopathy*. Lancet, 1982 : p. 725.

[10]. Chalovich, J. M., C. T. Brut, M. J. Danon, T. Glonek, and M. Barany, *Phosphodistress in Muscular Dystrophies*. Ann. N. Y. Acad. Scie, 1979. 317 : p. 649.

[11]. Chance, B., S. Eleff, and Jr. J. S. Leigh, *Non-invasive,Nondestructive Approaches to Cell Bioenergetics*. Proc. Nat. Acad. Sci. USA, 1980. 77 : p. 7430.

[12]. Misra , L .K., S. R. Kasturi, S.K. Kundu, Y. Harai, C. F. Haziewood , M.G. Luthra , S. W. Yamanashi, R.P. Munjal, S. R. Amety, *Evaluation of Muscle degeneration in inherited muscular Dystrophy by Nuclear Magnetic Resonance Techniques.* Magn .Reson. Imag, 1982. 1(2) : p. 75-79.

[13]. Bradbury, E. M., P. D. Cary, G. E. Chapman, C. Crane-Robinson, S. E. Danby, H. W. E., Rattle, M. Bublika, J. Palav, and F. J. Aviles, *Studies on the Role and Mode of Operation of the Very-Lysine-Rich Histone H1 (F1) in Eukaryote Chromatin.* The Conformation of Histone H, Eur. J. Biochem, 1975. 52 : p. 605.

[14]. Lee, A. G., N. J. M. Birdsal, and J. C. Metcalfe, *Measurement of fast Lateral Diffusion of Lipids in Vesicles and in Biological Membranes by ^{1}H Nuclear Magnetic Resonance*. Biochem, 1974, 12 : p. 1650-1659.

[15]. Chapman, B. E., S. S. Danyluk, and K. A. McLuchlem, *A Model for Collagen Hydration*, Proc. Roy. Soc. London, B, 1971, 178 : p. 465.

[16]. Wuthrich, K, *NMR Studies of Structure and Function of Biological Macromolecules*, Noble lecture 8, Dec, 2002 : p.235-267.

[17]. Kurosu, H, and T. Yamanobe, *Synthetic Macromolecules, In : Nuclear Magnetic Resonance*, G. A. Webb, Editor, The Royal Society of Chemistry, Cambridge, U. K., 2008. 37 : p. 293-326,

[18]. Prior, M. J. W., *NMR in Living Systems, In : Nuclear Magnetic Resonance*, G. A. Webb, Editor, The Royal Society of Chemistry, Cambridge, U. K., 2008. 37 : p. 327-356,

[19]. Jardetzky, O., *Determination of Macromolecular Structure and Dynamics by NMR, In: NMR in the Life Sciences, E. M. Bradbury, and C., Nicolini,* Editor ,Plenum Press, New York., 1986 : p.49-72.

[20]. Housnell, E, *NMR of Carbohydrates, lipids and Membranes, In : Nuclear Magnetic Resonance*, G. S. Webb, Editor, The Royal Society of Chemistry, Cambridge, U. K.,2008. 37 : p. 274-292.

[21]. Simpson, P. J, *NMR of Proteins and Nucleic Acids, In : Nuclear Magnetic Resonance*, G. S. Webb, Editor,The Royal Society of Chemistry, Cambridge, U. K., 2008. 37 : p. 257-273,

[22]. Consonni, R. and L. R. Cagliani, *Nuclear Magnetic Resonance and Chemometrics to Access Geographical Origin and Quality of Traditional Food Products*, In : Advances in Food and Nutritional Research. 2010. 59 : p. 87-164.

[23]. Adan, A., D. Kilian, and J. G. Warren, *Applications of Natural Abundance Carbon-13 NMR to Studies of Proteins and Glycoproteins,* In: NMR and Biochemistry, S. J. Opella, and P. Lu, Editor, Marcel Dekker, Inc., New York and Basel, 1979 : p. 31-50.

[24]. Talebpour, Z., H. R. Bijanzedeh, S. Haghoo, and M. Shamsipir, *^{1}H NMR Methods for Simultaneous Identification and Determination of Caffeine and Theophylline in Human Serum and Pharmaceutical Preparations*. Anal. Chem. Acta, 2004. 506 : p.97-104.

[25]. Wishrat, D., *NMR Spectroscopy and Protein Structure Determination. Application to Drug Discovery and Development*. Current Pharm. Biotech, 2005.6:p. 105-120.

[26]. Newman, R. J., P. J. Bore, L. Chan, D. G. Gadian, P. Styles, D. Taylor, and G. K. Radda, *Nuclear Magnetic Resonance Studies of Forearm Muscle in Duchenne Dystrophy*. Br. Med. J, 1982. 10 (284{6322}) : p. 1072-1074.

[27]. Sharma, U., S. Arti, M. C. Sharma, C. Sarkar, and N. R. Jaganathan, *Skeletal Muscle Metabolism in Duchenne Muscular Dystrophy (DMD) : an in-vitro Proton NMR Spectroscopy Study*. Magn.Reson.Imaging, 2003. 21(2) : p. 145-53.

[28] Matsummura, K., I. Nakano, N. Fukuda, H. Ikehiro, Y. Tateno, and Y. Aoki, *Duchenne Muscular Dystrophy Carriers Proton Spin–Lattice Relaxation Times of Skeletal Muscles on Magnetic Resonance Imaging.* Neuroradiology, 1989. 31 : p. 373-376.

[29]. Zochodne, D. W., W. J. Koopman, N. J. Witt, T. Thompson, A. A. Driedger, D. Gravelle, C. F. Bolton, Forearm P-31 Nuclear Magnetic Resonance Spectroscopy Studies in Occulopharyngeal Muscular Dystrophy. Can. J.Neurol.Sci, 1992. 19(2) : p. 174-179.

[30]. Sharma, U. , S. Atri, M. C. Sharma, C. Sarkar, and N. R. Jaganathan, *Biochemical Characterization of Muscle Tissue of Limb Girdle Muscular Dystrophy : an ^{1}H and ^{13}C NMR Study*, NMR. Bio medicine, 2003. 16(4) : p. 213-223.

[31]. Barbiroli, B., R. Funicellc, S. Lotti, P. Montagna, A.Ferlini, and P. Zanial, *^{31}P-NMR spectroscopy in Becker, Dystrophy and DMD/BMD Carriers.* Altered Rate of Phosphate Transport. J. Neurol. Sci, 1992. 109(2) p. 185-195.

[32]. Donald. P. Y., B. Peter, S. John, C.R.N. Claire, B. Willliam, and C. Britton, *^{31}P NMR Studies in Duchenne Muscular Dystrophy*. Neurology, 1987, 37(1) : p. 165-169.

[33]. Griffin, J. L., H. J. William, E. Sang, K. Clarke, C. Rae, and J. K. Nichola, *Metabolic Profiling of Genetic Disorders : A Multitissue ^{1}H Nuclear Magnetic Resonance Spectroscopic and Pattern Recognition Study into Dystrophic Tissue.* Analt. Biochem, 2001. 93 : p. 16-21.

[34]. Sharma, R., M. Rehani, and A. Agarwala, *Detection of Metabolites by Proton Ex vivo NMR, in vivo MR Spectroscopy Peaks and Tissue Content Analysis: Biochemical–Magnetic Resonance Correlation: Preliminary results.* Asia. Pacific. J. Life Sci, 2009. 3 (3) : p. 183-202.

[35]. Šuput, D., A. Zupan, A. Spe, and F. Demsar, *Magnetic Resonance Imaging of Muscular Dystrophies and Neuropathies*. B. A. M., 1992. 2(4) : p. 285-290.

[36]. Cady, E. B., R. D. Griffiths, and R. H. T. Edwards, The Clinical Use of Nuclear Magnetic Resonance Spectroscopy for Studying Human Muscle Metablosim. Int. J. Tech. Assesment in Health Care, 1985. 1(3) : p. 631-645.

[37]. Chance, B., D. P. Younkin, R. Kelley, W. J. Bank, H. D. Berkowit, Z. Argov, E. Donlon, B. Bode, K. McCully, N. M. R. Buist, N. Kennaway, and M. O. John, Magnetic Resonance Spectroscopy of Normal and Diseased Muscles. Am. J. Med. Gen, 1986, 25(4) : p. 659-679.

[38]. Michael, B., D. D. Donald, G. Gustav, M.W. William, and L. M. John, *Natural abundance ^{13}C NMR Spectra of Human Muscle, Normal and Diseased.* Mag. Res. Med, 1984. 1(1) : p. 30-43.

[39] Schreiber, A., W. L. Smith, V. Ionasescu, H. Zellweger, E. A. Franken, V. Dunn, and J. Ehrhardt, *Magnetic Resonance Imaging of Children with Duchenne Muscular Dystrophy. Paediat*. Radiol, 1987. 17 : p. 495-497.

[40]. Kaiser, W. A., W. Hartt, W. H. Sturm, B. C. Schalke, and E. Zeitler, *^{31}P NMR Spectroscopy of Muscular Diseases : Correlation with MR Imaging*. ROFO, 1987. 146(2) : p. 137-144.

[41]. Bottomley, P. A., Y. Lee, and R. G. Weiss, *Total Creatine in Muscle : Imaging and Quantification with Proton MR Spectroscopy.* Radiology, 1997. 204(2) : p. 403-410.

[42]. Garood, P., K.G. Hollingsworth, M.Eagle, B. S. Aribisala, D. Birchall, K. Bushby, and V. Straub, *MR Imaging in Duchenne Muscular Dystrophy : Quantification of T1–Weighted Signal, Contrast Uptake and the Effect of Exercise*. J.magn. Reson. Imaging, 2009 .Vol. 30(5) : p. 1130-1138.

[43]. Ogino, T., H. Ikehira, N. Arimizu, H. Mariya, K. Watimoto, S. Nishikawa, H. Shiratsuchi, H. Kato, F. Shishido, and Y. Tateno, *Serial Water Changes in Human Skeletal Muscles on Exercise Studied with Proton Magnetic Resonance Spectroscopy and Imaging.* Ann. Nucl. Med, 1994. 8(4) : p. 219-224.

[44]. Srivastava, N. K., S. Pradhan, B.Mittal, and G. A. N. Gowda, *High Resolution NMR Based Analysis of Serum Lipids in Duchenne Muscular Dystrophy Patients and its Possible Diagnostic Significance*. NMR. Biomedicine, 2010. 23(1) : p. 13-22.

[45]. Sarpel, G., J. L. Harry, J. D. Maris, and A. Omachi*, Erythocytes in Muscular Dystrophy Investigation with ^{31}P Nuclear Magnetic Resonance Spectroscopy.* Arch. Neurol, 1981. 28(5) : p. 271-274.

[46]. Bock, J. L, Analysis of Serum by High Proton Nuclear Magnetic Resonance. Clin. Chem, 1982. 28(9) p. 1873-1877.

[47] .Forbes, S. C., G. A. Walker, W. D. Rooney, D. I. Wang, S. Devos, J. Pollaro, W. Triplett, D. J. Lott, R. J. Willcocks, C. Senesac, M. J. Daniels, B. J. Byrne, B. Russman, R. S. Finkel, J. S. Meyer, H. L. Sweeney, and K.Vandenborne, *Skeletal Muscles of Ambulant Children with Duchenne Muscular Dystrophy : Validation of Multicenter Study of Evaluation with MR Imaging and MR Spectroscopy*. Radilogy, 2013. 269(1) : p. 198-207.

[48]. Hudson, L. and F. C. Hay, *Practical Immunology, 2nd edition, Black Well Scientific Publication*, Oxford, London, Edinburg, Boston, Melbourne, 1980:p. 22

[49]. Mandel, M., *Proton Magnetic Resonance Spectra of some Proteins Ribonuclease, Oxidized Ribonuclease Lysozyme and Cytochrome "C"*. J. Biochemistry, 1965. 240 (4) : p. 1586-1592.

[50]. Vitolis, C., and A. Weljie, *Identifying and Qualifying Metabolites in Blood Serum and Plasma,* Chenomx App Note, http://www.chenomx.com. 2006.: p.1-6.

[51]. Burton, D. R., *Paramagnetic Ions as Relaxation Probes in Biological Systems, In : ESR and NMR of Paramagnetic Species in Biological and Related Systems*. I. Bertini and R. S. Drago Editor, Reidel, Dordrecht, Holland, 1980 p. 151.

[52]. Mayer, M., *The Complement System, In : Immunology, Readings from Scientific American*, F. M. Burnet, Editor, W. H. Freeman, & Co., San Francisco, 1976. p. 143-155.

[53]. Huber, H., J. Deisenhofer, P. M.Colman, M. Matsushima, and W. Palm, *Crystallographic Structure of An IgG Molecule and Fc Fragment,* Nature, 1976. 264 : p. 415-420.

[54]. Boyd, J., S. B. Easterbrook-Smith, P. Zavodsky, C. Mountford-Wright, and R. A. Dwek, *Mobility and Symmetry in the Fc and pFc' Fragments as probed by ^{1}H NMR . Mol*. Immunol, 1979 , 16(11) : p. 851-8.

[55]. Cohen, J. S., L. J. Hughes, and J. B. Wooten, *Observations of Amino Acid Side Chain in Protein by NMR Methods, In : Magnetic Resonance in Biology,* J. S. Cohen, Editor 3, John Wiley & Sons, New York, Singapore, 1983. p. 130-247.

[56]. Kumar, A., G. Wagner, R. R. Ernst, and K. Wuthrich, *Build Up Roles of the Nuclear Overhouse Effects Measured by Two-Dimensional Proton Magnetic Resonance Spectroscopy : Implications for Studies of Protein Information.* J. Am. Chem. Soc, 1981 .103(13) : p. 3654-3658.

[57]. Nagayama, K. and K. Withruch, *Systematic Application of Two-Dimensional Nuclear Magnetic Resonance Techniques for Studies of Protein 1. Combined use of Spin-Echo-Correlated Spectroscopy and J-Resolved Spectroscopy for the Identification of Complete Spin Systems of Non-Labile Protons in Amino Acid Residues.* Eur. J. Biochem, 1981 . 114 :p. 365-374

[58]. Wagner, G., A. Kumar, and K. Wuthrich, *Systematic Application of Two-Dimensional ^{1}H Nuclear Magnetic Resonance Techniques for Studies of Protein 2. Combined Use of Correlated Spectroscopy and Nuclear Overhouse Spectroscopy for Sequential Assignment of Backbone Resonance and Elucidation of Polypeptide Secondary Structures.* Eur. J. Biochem , 1981. 114 : p. 375 .

[59]. Glick, R. E., D. F. Kates, and S. J. Ehrenson, *Applicability of the Macroscopic Magnetic Susceptibility Model to Solvent Effects in Nuclear Magnetic Resonance*. J. Chem. Phys, 1959. 31 : p. 567 .

[60]. Moure, R., and R. J. P. Williams, *Nuclear Magnetic Resonance Studies of Eukaryotic Cytochrome C Assignment of Resonance of Aromatic Amino Acids.* Eur. J. Biochem, 1980. 103 : p. 493-502.

[61]. Spera, S, and A. Bax, *Empirical Correlation between Protein Backbone Conformation and C Alpha and C Beta 13 Nuclear Magnetic Resonance Chemical Shifts*. J. Am. Chem. Soc, 1991. 113 : p. 5490-5492.

[62]. Kuszewski, J. Q., A. M. Gronenborn, and G. M. Clore, *The Impact of Direct Refinement against ^{13}C and ^{13}C Chemical shifts on Protein Structure Determination by NMR.* J. Mag. Res. B, 1995. 106 (1) : p. 92-96.

[63]. Withrat, D. S., and B. D. Sykes, *The ^{13}C Chemical Shift Index : A Simple Method for the Identification of Protein Secondary Structure using ^{13}C Chemical Shift Data*. J. Biomol. NMR, 1994. 4 : p. 171-180.

[64]. Wang, Y. J., and O. Jardetzky, *Probability Based Protein Secondary Structure Identification Using Combined NMR Chemical Shift Data.* Protein Sci, 2002. 11 : p. 852-861.

[65]. Cornilescu, G., F. Delaglic, and A. Bax, *Protein Backbone Angle Restraints from Searching A Data Base for Chemical Shift in a Sequence Homology.* J. Biomol. NMR, 1994. 13 : p. 289-302.

[66]. Cavalli, A., X.Salvatella, C. M. Dobson, and M. Vendruscola, *Protein Structure Determination from NMR Chemical Shifts. Proc.* Natl. Acad. Sci. USA. 2007. 104 : p. 9615-9620 .

[67]. Shen, Y., O. Lange, F. Delaglio, P. Rossi, J. M. Aramini, G. H. Liu, A. Eletsky, Y. B. Wu, K. K. Singarapu, A. Lemak, A. Ignatchenko, C. H.Arrowsmith, T. Szperski, G. T. Montelione, D. Baker, and A. Bax, *Consistent Blind Protein Structure Generation from NMR Chemical Shift Data*. Proc. Natl. Acad. Sci, USA, 2008. 105 : p. 4685-4690.

[68]. Withrat, D. S., A. D. Arndt, M. Berjanskii, P. Tang, J. Zhou, and G. Lin, *$CS_2$3D: Awes Server for Rapid Protein Structure Generation using NMR Chemical Shifts and Sequence Data*. Nucleic Acids Res, 2008. 36 : p. W496-W502 .

[69]. Montalvao, R. W., A. Cavalli, X., Aalvatella, T. L. Blundell, and M. Vendruscok, *Structure Determination of Protein and Protein Complexes using NMR Chemical Shifts : Case of An Endonuclease Colicin and Immunity Protein Complex.* J. Am. Chem. Soc, 2008. 130 (4) : p. 15990-15996.

[70]. Dominguez, C., D. Boelens, and A. M. J. J. Bonvin, *A Protein and Protein Docking Approach and Biochemical or Biophysical Information*. J. Am. Soc, 2003 . 125(7) : p. 1731-1737.

[71]. Satoshi, E. and Y. Arata, *Proton Nuclear Magnetic Resonance Study of Human Immunoglobulin G1 and their Proteolytic Fragments : Structure of the Hinge Region and Effects of A Hinge Region Deletion on Internal Flexibility.* Biochemistry, 1985. 24(6) : p. 1561-1568.

[72]. Koichi, K., C. S. Fridman, W. Yamada, K. Kabayashi, S. Uchiyama, H. H. Kim, J. Fenokizono, A. Galinha, Kobayashi, Y., Fridman, W. H., Y.Arata, and I. Shimada, *Structural Basis of the Interaction between IgG and Fcy Receptors*. J. Mol. Biol, 2000. 295(2) : p. 213-224.

[73]. Brab, A. W., and J. H. Prestegard, *MR Analysis Demonstrates Immunoglobulin GN-glycans are Accessible and Dynamic Nature.* Chemical Biol, 2011. 7 : p. 147-153.

[74]. Nicholson, L. K., L. E. Kay, D. M. Boldisseri, J. Arange, P. E. Young, A. Bax, D. A. Torchia, *Dynamics of Methyl Group in Proteins as studied by Proton Detected ^{13}C NMR Spectroscopy : Application to the Leucine Residues of Staphylococcal Nuclease.* Biochemistry, 1992. 31 : p. 5253-5263.

[75]. Szilagye, L., and O. Jardetzky, *Alpha Proton Chemical Shifts and Secondary Structure in Proteins*. J. Magn. Reson, 1989. 83 : p. 441.

[76]. Pastore, A, and U. Saudek, *The Relationship between Chemical Shift and Secondary Structure in Proteins*. J. Magn. Reson., 1990. 90 : p. 165-176.

[77]. Oldfield, E., *Chemical Shifts and Three Dimensional Protein NMR Structures*. J. Biomol, 1995. 5: p. 217-225.

[78]. Jardetzky, O., and C. D. Jardetzky, *Proton Magnetic Resonance Spectra of Amino Acids*. J. Biol. Chem, 1958. 233 : p. 383.

[79]. Cteighton,T.E , *Structure and Molecular Proteins* , In: Proteins , 2nd edition , W.H. Freeman and company , New York,1993: p. 238-244.

SOCIETY FOR SCIENCE AND EDUCATION
UNITED KINGDOM

JBEMi JOURNAL OF BIOMEDICAL ENGINEERING AND MEDICAL IMAGING

VOLUME 1, ISSUE 1

Objective evaluation of chronic laryngeal dysphonia by spectro-temporal analysis

S. Abdelouahed[1], M. Benabdallah[1], S. A. Aounallah[2], F. Hadj Allal[2]

[1]*Biomedical engineering laboratory, Tlemcen University, Algeria*

[2] *University Hospital of Tlemcen, Algeria*

[1]sara.abdelouahed@hotmail.com; m_benabdellah_2000@yahoo.fr

ABSTRACT

In this paper we develop a system dedicated to the objective characterization of dysphonia chronic laryngeal origin. The purpose of this system is threefold: diagnosis, treatment and monitoring of patient. . For this we proceed initially to the remote recording and archiving of an acoustic speech signal voiced in this case "a" sustained for three seconds. We then apply at the Otorhinolaryngology (ORL) department of the University Hospital of Tlemcen, different algorithms of objective assessment of three parameters in this case the fundamental frequency, Disturbance of short-term speech signal (jitter) and Short-Time discrete Fourier Transform (ST.DFT) that allow experts to assess the development of chronic dysphonia of tumor or inflammatory origin (larynx cancer, inflammatory polyp of the vocal cords, chronic laryngitis).

Keywords: Telemedicine; ST.DFT; Chronic dysphonia; Voiced sound; Jitter; Fundamental frequency.

1. INTRODUCTION

The voice is a spectacular indicator of physical and mental health of a person. The technology of voice pathology has been a marked increase over the past two decades, the voice processing is now a fundamental component of engineering [13] [1]. The special importance of voice processing in the more general framework is due to the privileged position of the speech as a vehicle of information in our human society. [11] The voice is indeed produced by the vocal tract, continuously monitored by the motor cortex [8] [4]. Among the voice treatment applications we distinguish [5] [6]:

1) Temporal spatio-spectro analysis of the vocal signal observing the objective characterization of dysphonia of laryngeal origins [9][10].

DOI: 10.14738/jbemi.11.69
Publication Date:15th February 2014
URL: http://dx.doi.org/10.14738/jbemi.11.69

2) Quantitative estimation of characteristics parameters of the vocal signal during its acoustical representation including the Fundamental Frequency and the jitter of voiced sounds [7] [12].

2. MATERIEL AND METHODS

The slide that we have implemented is composed of an interface for acquiring the acoustic speech signal consists of a dynamic microphone to reproduce sound in analog form and sound card for digitization and an environment software to archive the signal in Wave format in order to perform the calculation of different indices and we had to implement an algorithm for converting Wave format to decimal format in Visual Basic environment. The experimental protocol includes the following steps:

- Pronunciation of a voiced sound in this case 'a' sustained for three seconds.
- The division of the signal into 6 frames each 0.5 seconds
- The calculation of the three indices (spectral content, fundamental frequency and jitter) averaged over six frames.
- The correlation between the indices themselves and the balance sheet and para-clinic of patients.
- The implementation of an interactive database of physiological and pathological acoustic voice signals for a clinical and epidemiological study and better therapeutic management.

2.1 Global Algorithm of the application

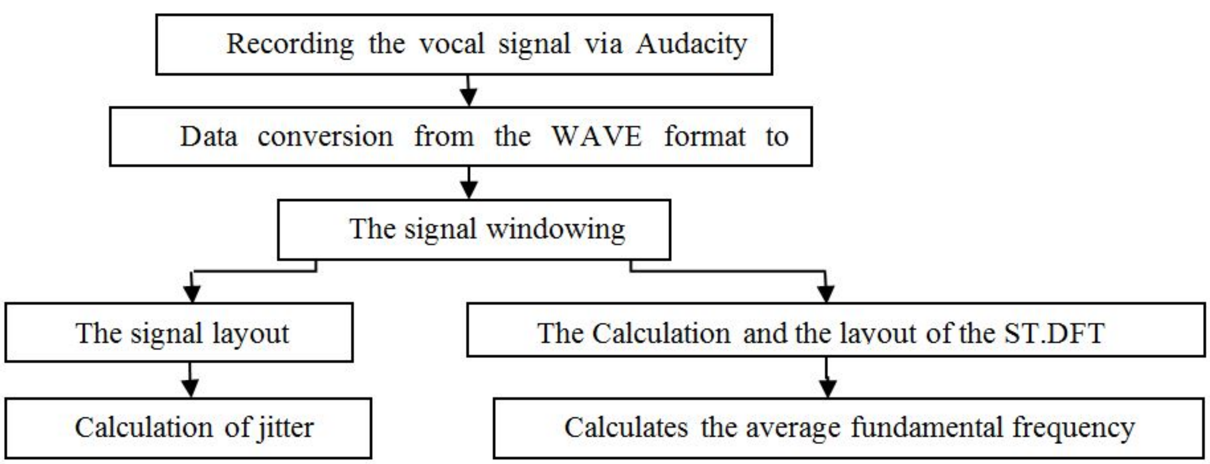

Figure 1: The algorithm

3. CLINICAL EVALUATION

3.1 Healthy subject study

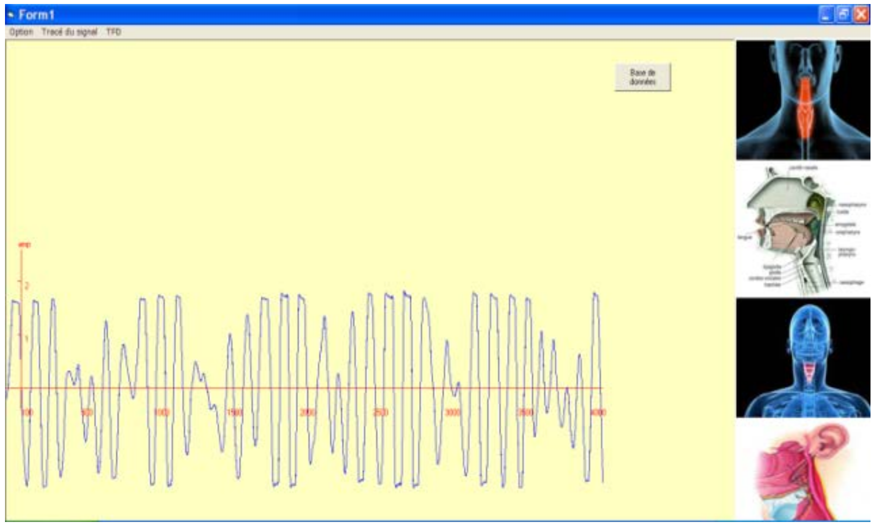

Figure2. Temporal layout of vocal signal of a healthy subject

Figure 3. Frequency layout of vocal signal of a healthy subject

The average fundamental frequency is: **200.60 HZ** and jitter is**: 0.69Sec**

The fundamental frequency established by gliding average method and jitter [3] is given by following equations:

$$F_0 = \frac{1}{N}\sum_{i=1}^{N} F_0^{(i)}$$

$$\text{jitter} = \frac{\frac{1}{N-1}\sum_{i=1}^{N-1}\left|T_s^{(i)} - T_s^{(i+1)}\right|}{\frac{1}{N}\sum_{i=1}^{N} T_s^{(i)}}$$

When N is the selection number (N=6).

3.2 Sick subjects

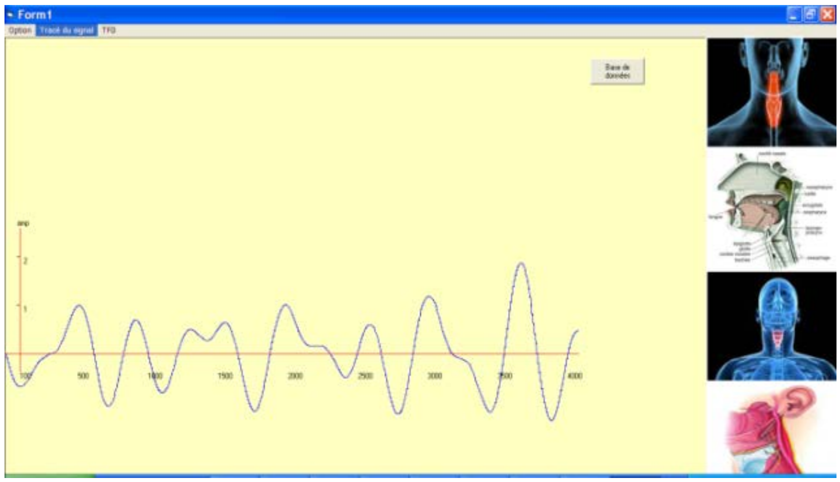

Figure 4: Temporal layout of patient attains a larynx cancer

Figure 5: Frequency layout of vocal signal of a patient whose attains a larynx cancer

The averaged fundamental frequency is: **62.48 HZ** and jitter is: **2.62.**

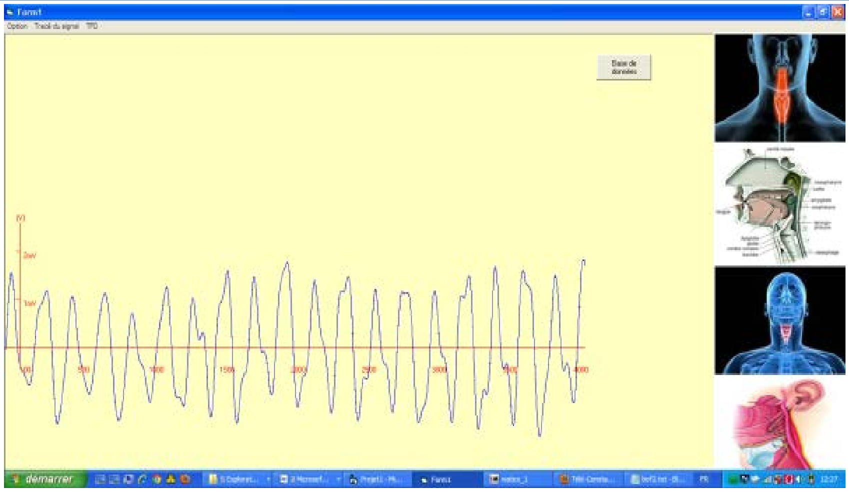

Figure 6: Temporal layout of patient attains an inflammatory polyp

Figure 7. Frequency layout of vocal signal of a patient whose attains a larynx cancer

The average fundamental frequency is: **118.80 HZ** and jitter is: **1.59 Sec**

3.2 Distant sustained of the patient:

The patient treated by the radiotherapy (persons suffering from cancer) or by medical treatment (a patient presents a clinical inflamed syndrome) and whose living in isolated area especially the north polar can be monitored remotely through the implementation of a platform at health centers proximities through periodical recording of the acoustical signal vocal according to the precedent described protocol and its O.R.L department of University Hospital accordance with the architecture client-server hold up by the component Winsock compatible with the protocol TCP/IP which permitted the transmission of the data toward intranet or internet thus the patient avoiding the inutile movement a condition that he responds favorably to the instituted treatment.

4. RESULTS

Table 1 : The jitter and the average fundamental frequency of healthy subjects

Healthy subjects										
Fundamental frequencies F0(HZ)	1st subject	2nd subject	3rd subject	4th subject	5th subject	6th subject	7th subject	8th subject	9th subject	10th subject
	Male								Female	
1st selection	227.05	200.65	190.09	184.81	216.49	205.93	184.81	211.21	200.65	190.09
2nd selection	184.81	211.2	184.8	211.21	184.81	179.53	205.93	190.09	211.2	184.8
3rd selection	184.81	184.8	184.8	179.53	200.65	221.77	227.05	195.37	184.8	184.8
4th selection	227.05	184.8	216.49	184.81	221.77	205.93	211.21	216.49	184.8	216.49
5th selection	195.12	211 .4	184.81	211.21	200.65	184.81	195.37	179.53	184.81	184.81
6th selection	184.8	195.37	211.21	184.8	184.81	205.93	195.37	195.37	195.37	211.21
The average fundamental frequencies (HZ)	200.6	198.03	196.68	192.72	201.53	200.65	203.29	198.01	193.59	195.36
Jitter (sec)	0.69	0.67	0.68	0.67	0.77	0.68	0.61	0.79	0.7	0.68

Table 2 : The jitter and the average fundamental frequency of sick subjects

Sick subjects										
Fundamental frequencies Fs (HZ)	1st subject	2nd subject	3rd subject	4th subject	5th subject	6th subject	7th subject	8th subject	9th subject	10th subject
	Larynx cancer						Inflammatory pathology			
1st selection	73.92	58.08	68.64	47.52	47.52	50.52	105.6	121.44	105.6	174.25
2nd selection	73.92	47.52	47.52	52.8	63.36	67.36	147.85	105.6	137.29	163.69
3rd selection	52.8	47.5	47.52	52.8	47.52	50.52	126.73	110.88	126.73	142.57
4th selection	73.92	42.24	68.64	47.58	58.08	58.08	142.57	100.32	110.88	174.81
5th selection	63.36	42.24	68.64	58.08	63.36	68.64	105.6	137.29	121.44	163.69
6th selection	73.92	47.52	73.92	58.08	68.64	47.52	110.88	137.29	105.6	142.57
The average fundamental frequencies (HZ)	68.64	47.51	62.48	52.81	58.08	57.10	123.20	118.8	117.92	160.17
Jitter (sec)	2.64	2.22	2.62	2.4	2.69	2.65	1.5	1.59	1.55	1.03

5. DISCUSSIONS

We notice that for the healthy subjects the fundamental frequency is about 200 Hz corresponding to the value of the physiological fundamental frequency of the vowel 'a' [14] and jitter is around 0.7 Sec. On the other hand it's reduced in the persons suffering from cancer it's situated around 60HZ and jitter extend to 2.5Sec. This diminution of the fundamental frequency and the augmentation of jitter are also present in the case of chronicle inflamed diseases of the larynx but a lower degree F_s around the interval 100-160 HZ and jitter around the interval 1-1.6 Sec .Even the extended spectral is lower in cancerous patients because of an important reduction notice Even the extended spectral is lower in cancerous patients because of an important reduction with a total absence of the vibrations of vocals cords . This limitation of the content of the frequency is also present but with a truncated manner in the case of chronicle inflamed diseases of larynx.

6. CONCLUSION

Characterization and objective assessment of chronic dysphonia were studied using three parameters. The fundamental frequency was around 120 Hz and the jitter was around 1.2 sec in cases of inflammatory disease, while the frequency was low at around 60 Hz and the jitter increased to 2.5 sec in larynx cancer, where the jitter was three times higher than healthy subjects. The clinical and para-clinical examinations, notably the pathological diagnosis, were in perfect agreement with the evolution of their indices. Clinical validation of the results is still subject to much larger samples supported by a rigorous statistical support.

ACKNOWLEDGEMENT

This work was done in collaboration with doctors in ORL, ORL department of the University Hospital Tlemcen.Algeria.

REFERENCES

[1]. A.Drygajlo, « Traitement de la parole »-Partie 1-, école Polytechniques Fédérale de Lausane EPFL, 1998.

[2]. L.Benlaldj, « Etude de la méthode PLP (Perceptual linear prediction) en reconnaissance automatique de la parole », Thèse de magister en électronique, spécialité : Signaux et Systèmes, promotion 1999/2000.

[3]. LAKHDAR Mohammed Hicham, HASSAM Ahmed, « classification des sons de la parole par la technique PLP », Mémoire de fin d'étude pour l'obtention du diplôme d'ingénieur d'état en contrôle, Université ABOU BEKER BELKIAD TELEMCEN ,2001.

[4]. Calliope, la parole et son traitement automatique, Ed. Masson, 1989.

[5]. T. Dutoit, « Introduction au Traitement Automatique de la Parole », Notes de cours, Faculté Polytechnique de Mons, 2000.

[6]. Dr. ANDRZEJ DRYGAJLO, « TRAITEMENT DE LA PAROLE », "Interactive Multimodal Information Management (IM)2" , Laboratory of IDIAP (LIDIAP) Institute of Electrical Engineering (IEL) ,Swiss Federal Institute of Technology

[7]. Dr Camille Finck, chapitre sur « L'évaluation fonctionnelle des dysphonie d'origine laryngé », Service d'Oto-rhino-laryngologie, CHU sart Tilman, Université de Liège, Liège, Belgium.

[8]. GHIO, A.; GIOVANNI, A.; TESTON, B.; RÉVIS, J.; YU, P.; OUAKNINE, M.; ROBERT, D.; LEGOU, T. Bilan et perspectives de quinze ans d'évaluation vocale par méthodes instrumentales et perceptives. Actes, Journées d'Etude sur la Parole (JEP) (27 : 2008 juin 9-13 : Avignon, FRANCE). . Avignon: LIA. 2008

[9]. GHIO, A.; POUCHOULIN, G.; GIOVANNI, A.; FREDOUILLE, C.; TESTON, B.; RÉVIS, J.; BONASTRE, J.-F.; ROBERT, D.; YU, P.; OUAKNINE, M.; GUARELLA, M.-D.; SPEZZA, C.; LEGOU, T.; MARCHAL, A. Approches complémentaires pour l'évaluation des dysphonies : bilan méthodologique et perspectives. Travaux Interdisciplinaires du Laboratoire Parole et Langage d'Aix-en-Provence (TIPA), vol. 26. 2008, p. 33-74.

[10]. YU P., GARREL R., NICOLLAS R., OUAKNINE M., GIOVANNI A., (2007), "Objective voice analysis in dysphonic patients. New data including non linear measurements", Folia Phoniatrica et Logopaedica, 59:20-30. Lausanne (EPFL).

[11]. Giovanni A., Yu P., Révis J., Guarella MD., Teston B., Ouaknine M. (2006). "Analyse objective des dysphonies avec l'appareillage EVA. Etat des lieux.", Revue Oto-Rhino-Laryngologie Française, 90, p3 183-192

[12]. TESTON, B. L'évaluation instrumentale des dysphonies. Etat actuel et perspectives. In Giovanni A. (ed.) Le bilan d'une dysphonie. ISBN 2-914513-62-3. Marseille: Solal. 2004, p. 105-169.

[13]. VIALLET, F.; TESTON, B. Objective evaluation of dysphonia: acoustic and aerodynamic methods. Proceedings of European Laryngological Society: Around dysphasia, dysarthria, dysphonia (2003: Toulouse, FRANCE). 2003, p. 53-55.

[14]. Emmanuelle Guibert, « Caractéristiques physiques et auditives d’un signal sonore

SOCIETY FOR SCIENCE AND EDUCATION
UNITED KINGDOM

JBEMi JOURNAL OF BIOMEDICAL ENGINEERING AND MEDICAL IMAGING

VOLUME 1, ISSUE 1

Recovery and processing of 3D images in X-ray tomography

V.I. Syryamkin, E.N. Bogomolov, V.V. Brazovsky, G.S. Glushkov

National Research Tomsk State University

ABSTRACT

The article is to study operating procedures of an X-ray micro tomographic scanner, and the module of reconstrusction and analysis 3D-image of the test sample in particular. An algorithm for 3D-image reconstruction based on the image shadow projections and mathematical methods of the processing are described. Chapter 1 describes the basic principles of X-ray tomography, general procedures of the device developed. Chapter 2 and 3 are devoted to the problem of resources saving by the system during the X-ray tomography procedure, what is achieved by preprocessing of the initial shadow projections. Preprocessing includes background noise removing from the images, which reduces the amount of shadow projections in general and increases the efficiency of the group shadow projections compression. Chapter 4 covers general procedures of defect search, which is based on the vector analysis principles. In conclusion, the main applications of X-ray tomography are presented.

Keywords: X-ray tomography, 3D-image analysis, 3D-reconstruction, data compression, background noise removing, defect search.

1. INTRODUCTION

Modern manufacturing, including production and application of medical equipment and devices, require adequate methods of diagnostic quality control of structure of organic and inorganic topologically and compositionally heterogeneous objects. Detection and precise localization of defects are the main advantages of X-ray micro tomographic control [1].

X-Ray micro tomography is a layer-by-layer method of study of the internal structure of an object with the aid of multiple radiographic X-rays in different directions, followed by 3D-reconstruction recovery and processing of images. Scanning visualizes the entire internal 3D structure of the object, keeping it safe for other types of research. High-resolution of the model received is another advantage of the X-ray micro tomographic scanning method.

X-Ray micro tomographic scanner developed by the research group of Tomsk State University is designed to study the spatial structure of materials and crystals with a resolution of 1-13 microns.

DOI: 10.14738/jbemi.11.102
Publication Date:15th February 2014
URL: http://dx.doi.org/10.14738/jbemi.11.102

2. BASIC PRINCIPLES OF X-RAY MICRO TOMOGRAPHIC SCANNING

After installation of the test sample on the desktop (working area) of the scanner and giving a command for 3D recovery by an operator the system starts processing.

The desktop, with the sample on it, begins to rotate. At the same time the capture device of shadow projections with fixed frequency, connected with the rotation angle of the desktop, takes pictures of shadow projections and transmits the data to the working (memory) storage.

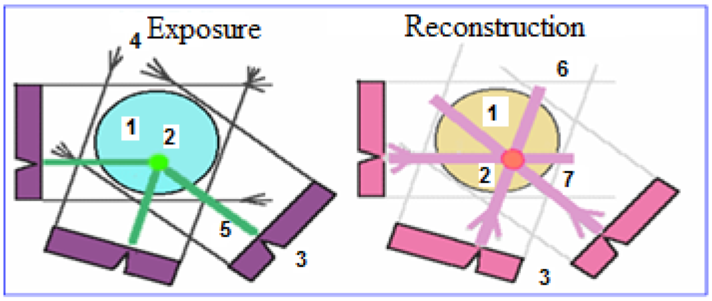

Figure 1. Diagrammatic view of the three different positions of the absorbing area and the reconstruction of the shadow projections received

In Figure1,

1 - Sample

2 – Heterogeneity area

3 - Capture device of shadow projections

4 - X-ray direction

5 – Projection lines of the heterogeneity area

6 - Lines of the sample recovery boundaries

7 – Lines of heterogeneity area recovery .

Central processing unit copies the information into the selected area of memory storage for images of shadow projections received and starts the process of multithreading computing via nVidiaTesla graphic module for removing noise on shadow projections images and projections and for the compression in the archive file.

In each new position of the object the lines of possible positions of the object are added to the reconstructed field in accordance with the position of the shadow projections (back projecting). After a few turns, the position of the absorbing area can be localized. With an increasing number of shadow projections in different directions, this localization becomes clear (Figure 2) [3].

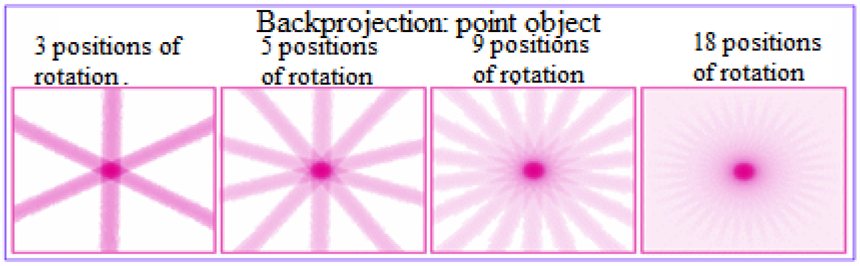

Figure 2. Reconstruction of a point object by means of a different number of displacements

3. BACKGROUND NOISE REMOVING FROM THE IMAGES

Removing background noise is an important function of the image processing, which allows to replace homogeneous background areas with single color in order to improve final image compressibility. Finding areas of the image corresponding to the background, allows to get rid of the data containing no useful information.

In practice, the images of the shadow projections are very noisy. The main noise sources - inhomogeneous X-ray tube radiation and the residual luminescence of the detector screen. As a consequence, the image of shadow projections, both in the background and in the shadow areas of the object have a wide range in the brightness level. The basic idea of a method determination the area of the image corresponding to the background noise, is to break the image into sections and then analyze its sites.

Operating mode of the tomographic scanner includes such specifications as:

1) The density of pixels and the resolution of the detector;

2) Radiation power X-ray tube;

3) Filters (generally aluminum or copper ones) and the materials applied.

The specifications calculated are:

1) The minimum brightness of the pixel;

2) The maximum brightness of the pixel;

3) The average brightness of the pixel;

4) The mean square deviation of the pixel brightness.

To improve the speed and quality of background noise removal it is convenient to define a boundary value of pixel brightness the way it will be possible to interpret any point of greater brightness as background and replace it with the highest possible brightness value (65535 for 16-bit color) . If you select the minimum brightness as the boundary brightness for the points of the background area, a small part of the background noise belonging to border areas of the object will remain on the image, as the area close to the boundary is noisier than in the background.If you select maximum brightness as boundary brightness of the object, then some part of the image pixels belonging to the object on the border with the background will be interpreted as background and replaced with the maximum brightness.

Due to the statistical averaging, both ways for removing pixels may lead to the same results (in terms of accuracy required for reconstruction) and improve the quality of reconstruction.

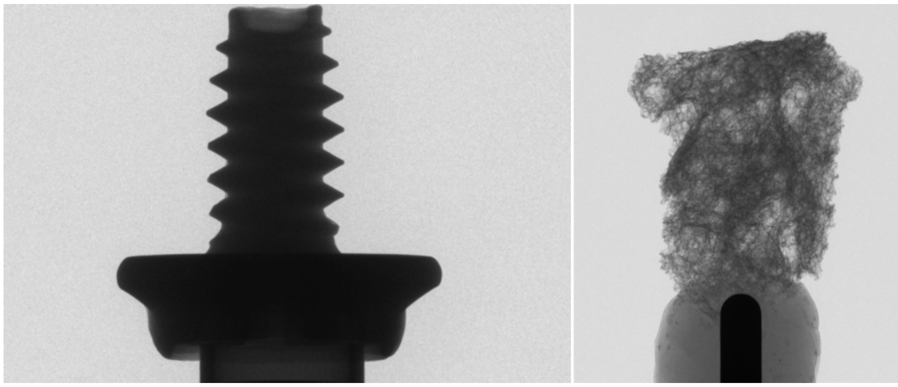

Figure 3 – Illustration of shadow projections.

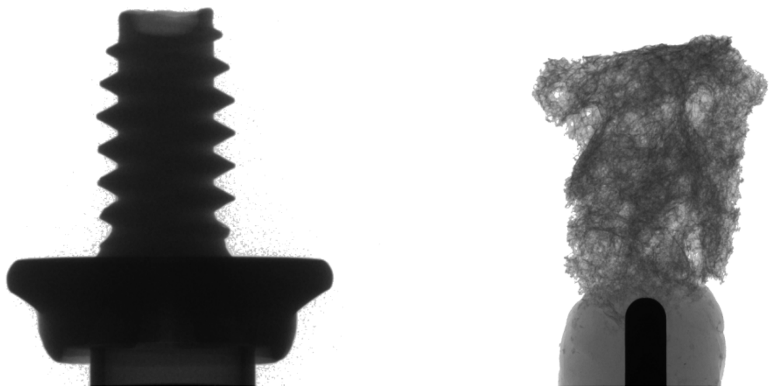

Figure 4 – Shadow projection images after the removal of background noise.

Figure 2 shows the typical images of shadow projections received using an X-ray micro tomographic scanner, Figure 3 - modified images with background noise removed. [2,3].

4. DATA COMPRESSION

There are various methods of data compression without sacrificing. The fastest and easiest to implement is RLE- compression: coding of the series of repeated values, which can be done in one pass. [4,5]

If the original image is represented by a sequence of double-byte characters (16 bits), the values of which range from 0 to 65535, then after the construction of the difference each point must be encoded by 17 bits, as the values must range from - 65535 to 65535.

Original image occupies $P_0 = 2 * W * H$ bytes of information, where W and H - number of dots (pixels) horizontally and vertically. Transformed image, in which each pixel is encoded with i number of bits, will occupy the following number of bytes:

$$P_i = W * H * \frac{i}{8}.$$

Points, the storage of which require more than i bits, are entered into delete set, which takes E = 2 (N-N_i) bytes. The total volume of the transformed data:

$$S_i = W * H * \frac{i}{8} + 2(N - N_i).$$

Thus, the required number of bits j, which is required to encode the image is $S_j = \min(S_0,\ S_1, \dots, S_{17})$.

Image preprocessing module connects with other modules through the integrated management environment and provides the undistorted compression and decompression of the images received on the X-ray micro tomographic scanner .

5. 3D-RECONSTRUCTION ANALYSIS

After completion of the 3D- reconstruction the central processing unit determines the user-visible areas of 3D- reconstruction, reads data from the hard disk (RAM) and sends to the graphic module for visualization and display on the screen. 3D- reconstruction requires a large number of high resolution images of the sample, which needs a computer system with advanced performance and capacity of memory resources for storing and processing the data. There are various methods for the automatic search of defects that give acceptable results for certain objects under study. Gradient analysis method allows to search defects in the density of quite homogeneous non-biological objects [5, 6]. Initial data for gradient analysis method is the density values array at each point of the sample, which determine the material density distribution function ρ (x, y, z), thus the gradient field of the sample can be constructed. Defects will be determined by inhomogeneity of the field, that is, the presence of density gradients:

$$\nabla\rho(x, y, z) = (\frac{\partial\rho}{\partial x}, \frac{\partial\rho}{\partial y}, \frac{\partial\rho}{\partial z}).$$

The image gradient $f(x, y)$ is defined at the point (x, y) as two-dimensional vector

$$G[f(x, y)] = \begin{bmatrix} G_x \\ G_y \end{bmatrix} = \begin{bmatrix} \frac{df}{dx} \\ \frac{df}{dy} \end{bmatrix}.$$

As it can be seen from vector analysis the vector G indicates the direction of maximum change of function f at point (x, y):

$$G[f(x, y)] = [G_x{}^2 + G_y{}^2]^{1/2} = [\left(\frac{\partial f}{\partial x}\right)^2 + \left(\frac{\partial f}{\partial y}\right)^2]^{1/2}.$$

Location based on the volume of these gradients can determine the size and nature of the defects.

The size and structure of the defects can be detected by the means of 3D location of the gradients.

Advantages of this method:

- Possibility to identify the type of defect;
- Possibility to determine the localization of the defect
- Possibility to identify the geometric and physical characteristics of the defect [7].

The proposed algorithms are used to achieve high degree detailing and accuracy of reconstruction and analysis of 3D-models (Figure 5):

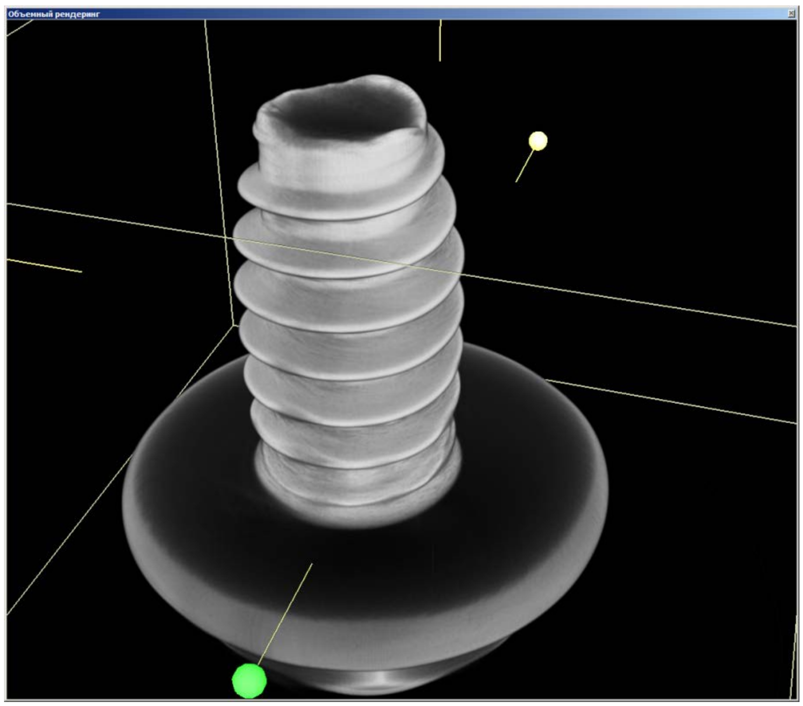

Figure 5 – 3D reconstruction

6. CONCLUSION

X-ray micro tomographic imaging for non-destructive testing for the technological and scientific purposes to study the internal structure of organic and inorganic objects in the following industries:

- in metallurgy for assessing the quality and structure of manufactured products;
- in machinery manufacturing and instrument engineering for quality control of the parts assembled;
- in the electronics industry for semiconductor assembly control and soldering electronic components with printed circuit boards;
- in physics for experiments carried out to visualize the internal structure of objects and physical processes of the samples [8];
- in biology and medicine for the optimization of X-Ray testing and diagnosis methods [9];

- in chemistry to visualize the internal structure of test samples, to observe the mechanism of the appearance of defects, to design and investigate new materials [2,10].

ACKNOWLEDGEMENT

Described methods form the image preprocessing module of the X-Ray micro tomographic scanner software, developed with the support of the Ministry of Education and Science in the framework of the Federal special purpose program of the Russian Federation (State contract № 16.523.11.3009).

REFERENCES

[1]. Marusina M. Ya., Kaznacheeva A.O. Modern methods of tomography. Textbook. St. Petersburg: St. Petersburg State University of Information Technologies, Mechanics and Optics Press, 2006.132 p.

[2]. Bubenchikov M.A., Gazieva E.E., Gafurov A.O., Glushkov G.S., Zhdanov D.S., Sankov D.V., Syryamkin V.I., Shidlovsky S.V., Yurchenko A.V. Modern methods of materials and nanotechnologies research. Tomsk: Tomsk State University Press, 2010. 366 p.

[3]. Tereshchenko S.A. Methods of computerized tomography. Moscow. Physics, mathematics and technical literature press 2004. 318 p.

[4]. Norenkov I.P. Principles of computer-aided design: Textbook for university students. 2nd edition. Moscow: Moscow State Technical University n.a. Bauman N.E., 2002. – 336 p.

[5]. Gorelik S.S., Rastorgouev L.N., Skakov Yu.A. X-ray and electron-optical analysis. 2nd edition. Moscow: Publishing house "Metallurgy", 1970. 366 p.

[6]. Syryamkin V.I., Zhdanov D.S., Borodin V.A., Metrology, diagnostics and certification of materials. Tomsk: Tomsk State University Press, 2011. 114 p.

[7]. Bogomolov E.N., Bubenchikov M.A., Gafurov A.O., Glushkov G.S., Gorbachev S.V., Zhdanov D.S., Osipov A.V., Syryamkin V.I., C Shidlovsky S.V., Yurchenko A.V. Modern methods of materials and nanotechnologies research. (Laboratory course). Tomsk: Tomsk State University Press, 2012. 412 p.

[8]. Eric F. Hequet, Ajay Pai Recognition of Cotton Contaminants via X-ray Microtomographic Image Analysis / International Textile Centre Texas Tech University and Electrical and Computer Engineering Texas Tech University URL: http://b-dig.iie.org.mx/BibDig/P03-0754/DATA/08P5.PDF

[9]. Maire E., Buffièr J. Y., Salvo L., Blandin J. J., Ludwig W., Létang J. M.On the Application of X-ray Microtomography in the Field of Materials Science/ Wiley Online Library. URL: http://onlinelibrary.wiley.com/doi/10.1002/1527-2648%28200108%293:8%3C539::AID-ADEM539%3E3.0.CO;2-6/abstract;

[10]. Fu Xiaowei, Elliot A. J., Bentham C., Hancock B., Cameron E.R., Application of X-ray Microtomography and Image Processing to the Investigation of a compacted Granular System / Wiley Online Library. URL: http://people.pwf.cam.ac.uk/jae1001/CUS/research/pfizer/Fu_etal_PPSC_2006.pdf.